

The $\mathbb{H}\mathbb{R}$ -Calculus: Enabling Information Processing with Quaternion Algebra

Danilo P. Mandic, Sayed Pouria Talebi, Clive Cheong Took,
Yili Xia, Dongpo Xu, Min Xiang, and Pauline Bourigault

ABSTRACT

From their inception, quaternions and their division algebra have proven to be advantageous in modelling rotation/orientation in three-dimensional spaces and have seen use from the initial formulation of electromagnetic field theory through to forming the basis of quantum field theory. Despite their impressive versatility in modelling real-world phenomena, adaptive information processing techniques specifically designed for quaternion-valued signals have only recently come to the attention of the machine learning, signal processing, and control communities. The most important development in this direction is introduction of the $\mathbb{H}\mathbb{R}$ -calculus, which provides the required mathematical foundation for deriving adaptive information processing techniques directly in the quaternion domain. In this article, the foundations of the $\mathbb{H}\mathbb{R}$ -calculus are revised and the required tools for deriving adaptive learning techniques suitable for dealing with quaternion-valued signals, such as the gradient operator, chain and product derivative rules, and Taylor series expansion are presented. This serves to establish the most important applications of adaptive information processing in the quaternion domain for both single-node and multi-node formulations. The article is supported by Supplementary Material, which will be referred to as SM.

I. INTRODUCTION

For the best part of ten year Sir William Rowan Hamilton concerned himself with constructing a framework for modelling three-dimensional spaces in a manner analogous to that achieved through complex-valued algebra for two-dimensional spaces. This came to fruition on the 16th of October 1843, when he derived the fundamental elements of what is known today as the quaternion algebra and carved the formula onto Brougham Bridge [1]. This focus on deriving a model for three-dimensional spaces, resulted in an algebra that is most effective in modelling real-world phenomena in our three-dimensional surroundings. Moreover, the resulting quaternion algebra itself is a four-dimensional one. Hamilton himself surmised of

the use of quaternions for simultaneous modelling of space and time in a letter to Sir John Herschel [2], writing; “*... how the one of time, of space the three, might in the chain of symbols girdled be. It is not so much to be wondered at, that they should have let me to strike out some new lines of research, which former methods have failed to suggest.*” Indeed, quaternions have seen use in quantum mechanics where, as one example, the quaternion four dimensional algebra allows to simultaneously formulate rotational and compression gradients [3,4]. The more recent use of quaternions for representing quantum fields is somewhat akin to that used for modelling electromagnetic fields by James Clark Maxwell [5], one of the main proponents for use of quaternion algebra over vector algebras [1].

Modern applications of the high dimensional division algebra that quaternions provide include multi-phase power systems [6,7], body motion tracking [8], sound processing [9,10], colour image processing [11], communication techniques that adopt space-time-polarisation multiplexing [12,13], and quantum computing [14]. Before the discussion on quaternions, their associate division algebra, and the $\mathbb{H}\mathbb{R}$ -calculus, it is important to introduce the nomenclature.

Nomenclature: Scalars, column vectors, and matrices are denoted respectively by lowercase, bold lowercase, and bold uppercase letters, while uppercase bold italic letters denote multivariate random processes, with calligraphic letters used to denote sets. The reminder of nomenclature is summarised as follows:

\mathbb{N}	natural numbers
\mathbb{R}	real-valued numbers
\mathbb{R}^+	positive real-valued numbers
\mathbb{C}	complex numbers
\mathbb{H}	quaternion numbers
\wedge	logical conjunction
$\Re(\cdot)$	operator returning the real component
$\Im(\cdot)$	operator returning the imaginary component
$\{\iota, \jmath, \kappa\}$	orthonormal imaginary units spanning the imaginary subspace of \mathbb{H}
$\Im_\chi(\cdot)$	operator returning the imaginary component alongside $\forall \chi \in \mathbb{H} \wedge \chi^2 = -1$
$\langle \cdot, \cdot \rangle$	inner product operator
\times	outer product operator
$(\cdot)^*$	conjugate operator
$\ \cdot\ $	second-order norm

$(\cdot)^T$	transpose operator
$(\cdot)^H$	transpose Hermitian operator
e	Euler's number
$E\{\cdot\}$	statistical expectation operator
$\Phi_\chi(\cdot)$	characteristic function of a random vector χ
∂	partial differential operator
d	total differential operator
∇_χ	gradient operator with respect to χ
$\mathcal{O}(\cdot)$	order of computational complexity
$\text{tr}\{\cdot\}$	trace operator
I	identity matrix of appropriate size
$\text{diag}\{\cdot\}$	constructs a block-diagonal matrix from its entries
$\rho\{\cdot\}$	spectral radius operator

A. Quaternion Algebra

A quaternion variable $q \in \mathbb{H}$, consists of a real part, $\Re(q)$, and a three-dimensional imaginary part, $\Im(q)$. In order to express $\Im\{q\}$ in the imaginary subspace of \mathbb{H} , three orthonormal imaginary units that span this space need to be selected. These units are generally denoted by $\{\iota, \jmath, \kappa\}$ and admit the product rules

$$\iota\jmath = \kappa, \quad \jmath\kappa = \iota, \quad \kappa\iota = \jmath, \quad \iota^2 = \jmath^2 = \kappa^2 = \iota\jmath\kappa = -1. \quad (1)$$

In this setting, a quaternion $q \in \mathbb{H}$ can be expressed as

$$q = \Re\{q\} + \Im\{q\} = \Re\{q\} + \Im_\iota\{q\} + \Im_\jmath\{q\} + \Im_\kappa\{q\} = q_r + \iota q_\iota + \jmath q_\jmath + \kappa q_\kappa$$

where $\{q_r, q_\iota, q_\jmath, q_\kappa\} \subset \mathbb{R}$.

The product of $q_1, q_2 \in \mathbb{H}$ can be found through component-wise multiplication of their real-valued constituents using the product rules in (1) and can be alternatively formulated using the inner product, $\langle \cdot, \cdot \rangle$, and the outer product, \times , as

$$q_1 q_2 = \Re(q_1)\Re(q_2) + \Re(q_1)\Im(q_2) + \Re(q_2)\Im(q_1) + \Im(q_1) \times \Im(q_2) - \langle \Im(q_1), \Im(q_2) \rangle. \quad (2)$$

Remark 1. Selection of the orthonormal units that span the imaginary subspace of \mathbb{H} is not unique. Indeed, a convenient change of these units can be used to simplify derivation/analysis

of quaternion-valued adaptive processing techniques, see [6,7,15] and SM-9A.

Remark 2. As a direct consequence of (1), product operations are not commutative in the quaternion domain, unless under an exceptional case. From (2), note that if q_1 and q_2 have parallel imaginary parts, by definition $\Im(q_1) \times \Im(q_2) = 0$ and thus the product becomes commutative. In essence, under this circumstance, q_1 and q_2 lie in a subspace of \mathbb{H} spanned by the real axis and the imaginary segment of q_1 (or equivalently q_2). This subspace admits a complex-valued algebra, making the multiplication commutative. In general, $\forall q_1, q_2 \in \mathbb{H} : q_1 q_2 = (q_2^* q_1^*)^*$.

The quaternion conjugate is defined as $q^* \triangleq \Re(q) - \Im(q)$, which allows for an inverse to be defined as

$$\forall q \in \mathbb{H} \setminus \{0\} : q^{-1} = \frac{q^*}{\|q\|^2}$$

with $\|q\|$ denoting the second-order norm of q , that is, $\|q\| = \sqrt{qq^*} = \sqrt{q_r^2 + q_i^2 + q_j^2 + q_\kappa^2}$.

B. Involution and the Augmented Representation

Strictly speaking, an involution is defined as a mapping that is its own inverse. However, a richer construct has been shown to be useful in the context of quaternions [16]. For the purposes of this article, an involution is defined as [16]

$$\forall q, \zeta \in \mathbb{H} \wedge \{\Re\{\zeta\} = 0, \|\zeta\| \neq 0\} : q^\zeta \triangleq \zeta q \zeta^{-1} \quad (3)$$

and is referred to as the involution of q around ζ . The definition in (3) is selected as it will allow the real-valued components of quaternions to be expressed using the linear and invertible mapping¹ [17,18]

$$\underbrace{\begin{bmatrix} \mathbf{q} \\ \mathbf{q}^i \\ \mathbf{q}^j \\ \mathbf{q}^k \end{bmatrix}}_{\mathbf{q}^a} = \underbrace{\begin{bmatrix} \mathbf{I} & \imath\mathbf{I} & \jmath\mathbf{I} & \kappa\mathbf{I} \\ \mathbf{I} & \imath\mathbf{I} & -\jmath\mathbf{I} & -\kappa\mathbf{I} \\ \mathbf{I} & -\imath\mathbf{I} & \jmath\mathbf{I} & -\kappa\mathbf{I} \\ \mathbf{I} & -\imath\mathbf{I} & -\jmath\mathbf{I} & \kappa\mathbf{I} \end{bmatrix}}_{\mathbf{A}} \begin{bmatrix} \mathbf{q}_r \\ \mathbf{q}_i \\ \mathbf{q}_j \\ \mathbf{q}_\kappa \end{bmatrix} \quad (4)$$

where \mathbf{q}^i , \mathbf{q}^j , and \mathbf{q}^k , denote the element-wise implementation of the involution, $\mathbf{A}^{-1} = \frac{1}{4}\mathbf{A}^H$, and \mathbf{q}^a is referred to as the augmented quaternion vector.

¹The quaternion conjugate can also be formulated using involutions as $q^* = \frac{1}{2}(q^i + q^j + q^k - q)$.

Finally, in a similar manner to complex-valued numbers, a quaternion $q \in \mathbb{H}$ can be expressed by its polar presentation as [15]

$$q = \|q\|e^{\xi\theta} = \|q\|(\cos(\theta) + \xi \sin(\theta)) \quad \text{where} \quad \xi = \frac{\Im(q)}{\|\Im(q)\|} \quad \text{and} \quad \theta = \text{atan}\left(\frac{\|\Im(q)\|}{\Re(q)}\right).$$

Thus, it follows that $\sin(\cdot)$ and $\cos(\cdot)$ functions can be expressed as

$$\sin(\theta) = \frac{1}{2\xi} (e^{\xi\theta} - e^{-\xi\theta}) \quad \text{and} \quad \cos(\theta) = \frac{1}{2} (e^{\xi\theta} + e^{-\xi\theta}) \quad (5)$$

with $\xi^2 = -1$.

C. Three-Dimensional Rotations

The attitude of a body after having foregone a rotation can be presented using a single right-hand rotation of that body by an angle of θ degrees about an axis η parallel to the direction that is unchanged by the rotation [15]. As shown in Fig. 1, the three-dimensional Cartesian coordinate system can be considered as representing the imaginary sub-space of a quaternion skew field, so that $\eta = (\eta_x, \eta_y, \eta_z)$ can be presented as $\eta = i\eta_x + j\eta_y + k\eta_z$. In this setting, the vector presetting the pre- and post-rotation orientation of the object, q_{pre} and q_{post} , are related as

$$q_{\text{post}} = \mu q_{\text{pre}} \mu^{-1} \quad \text{with} \quad \mu = e^{\eta \frac{\theta}{2}} = \cos\left(\frac{\theta}{2}\right) + \eta \sin\left(\frac{\theta}{2}\right). \quad (6)$$

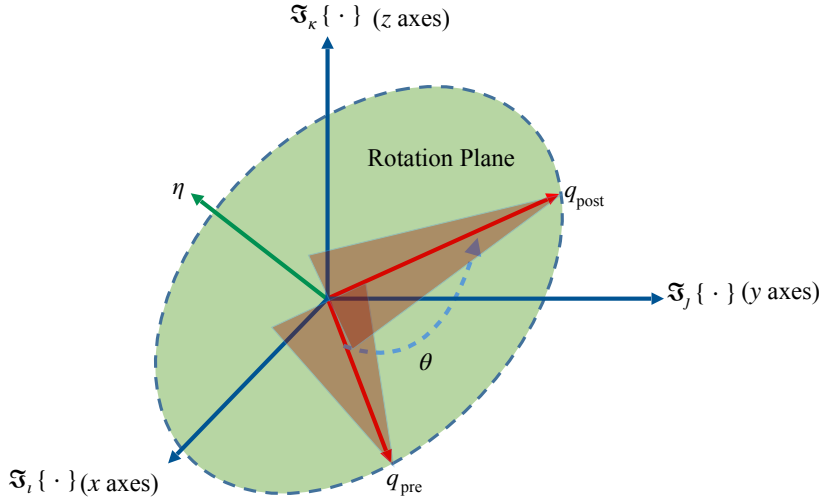


Fig. 1. Schematic of a rotation around η by an angle of θ , with q_{pre} and q_{post} pointing to the pre- and post-rotation orientation of the object in question.

Remark 3. The quaternion representation of rotations, as compared to Euler angles and real-valued rotation matrix algebras, holds a number of advantages. First, real-valued rotation

matrices lose a degree of freedom as one of the rotation angles reaches $\frac{\pi}{2}$ [15]. However, this is not the case for quaternions, where only the angle and the axis of rotation are required. Second, real-valued rotation matrices must have a unit determinant. This is hard to guarantee after many rotations have been computed due to the finite accuracy of computer operations. This problem does not arise in the quaternion representation [15,19].

Remark 4. Importantly, there seems to be an inherent relation between the formulation in (6) and the algebraic Lyapunov and Riccati recursions, two of the most fundamental equations in adaptive signal processing and control [20]. This is explored in SM-1. Moreover, in Example 1, we show how to leverage the division algebra of quaternions to model/track status of qubits.

Example 1. Quaternion-Valued Model of Qubits

In quantum computing, the fundamental unit of information is referred to as a quantum bit or qubit. A qubit, generally speaking, is a superposition of two bases denoted with $|0\rangle$ and $|1\rangle$ that are orthogonal to one another and represent state of quantum particle, e.g., up or down spin of an electron. The qubit can be in any superposition that satisfies

$$\forall\{\alpha, \beta\} \subset \mathbb{C} \wedge \|\alpha\|^2 + \|\beta\|^2 = 1 : |\psi\rangle = \alpha|0\rangle + \beta|1\rangle$$

where $|\psi\rangle$ represents state of the qubit while $\|\alpha\|^2$ and $\|\beta\|^2$ correspond to the probability of finding the quantum particle in state $|0\rangle$ or $|1\rangle$. Although use of two complex-valued variables α and β might suggest four degrees of freedom for $|\psi\rangle$, the condition, $\|\alpha\|^2 + \|\beta\|^2 = 1$, limits the degrees of freedom to three. Thus, the state of $|\psi\rangle$ can be described via a pure imaginary quaternion as demonstrated in Fig. 2 where

$$|\psi\rangle \leftrightarrow q = \iota \sin(\theta) \cos(\phi) + \jmath \sin(\theta) \sin(\phi) + \kappa \cos(\theta) \quad (7)$$

with θ and ϕ referring to the angles of $|\psi\rangle$ with the state $|\psi\rangle = |0\rangle$, corresponding to $\Im_\kappa\{q\}$, and angle between the state $\frac{1}{\sqrt{2}}(|0\rangle + |1\rangle)$, corresponding to $\Im_\iota\{q\}$, with projection of $|\psi\rangle$ onto the plane denoted $\left\{ \frac{1}{\sqrt{2}}(|0\rangle + |1\rangle), \frac{1}{\sqrt{2}}(|0\rangle + \iota|1\rangle) \right\}$, corresponding to the plane denoted by $\{\Im_\iota\{q\}, \Im_\jmath\{q\}\}$. In general, an operation of a quantum computer correspond to manipulations of the quantum state (groups of quantum states). These operations are effectively modelled in the quaternion domain using state-space and $\mathbb{H}\mathbb{R}$ -calculus tools. For more on this issue see SM-9E.

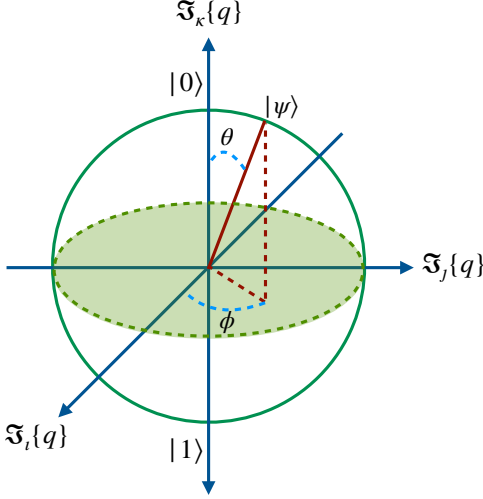


Fig. 2. A qubit representation with Bloch sphere, where $|\psi\rangle \leftrightarrow q = \iota \sin(\theta) + \jmath \sin(\theta) \cos(\theta) + \kappa \sin(\theta) \cos(\theta)$.

D. Introduction to Quaternion Statistics

Consider the quaternion-valued random process \mathbf{Q} , the statistical description of which is discernible from the joint characteristic function of its real-valued components given as

$$\Phi_{\mathbf{Q}}(\mathbf{s}_r, \mathbf{s}_i, \mathbf{s}_j, \mathbf{s}_\kappa) = \mathbb{E} \left\{ e^{\xi(\mathbf{s}_r^T \mathbf{q}_r + \mathbf{s}_i^T \mathbf{q}_i + \mathbf{s}_j^T \mathbf{q}_j + \mathbf{s}_\kappa^T \mathbf{q}_\kappa)} \right\}. \quad (8)$$

where $\xi \in \mathbb{H} \wedge \xi^2 = -1$. By exploiting the relation in (4), the characteristic function in (8) is expressed directly in the quaternion domain as

$$\Phi_{\mathbf{Q}^a}(\mathbf{s}^a) = \mathbb{E} \left\{ e^{\xi \Re\{\mathbf{s}^T \mathbf{q}\}} \right\} = \mathbb{E} \left\{ e^{(\frac{\xi}{4} \mathbf{s}^{aH} \mathbf{q}^a)} \right\} \quad (9)$$

with $\mathbf{s} = \mathbf{s}_r + \iota \mathbf{s}_i + \jmath \mathbf{s}_j + \kappa \mathbf{s}_\kappa$. Since (9) uses the quaternion random vector in its augmented form, it is referred to as the augmented quaternion characteristic function (AQCF) [15]. This terminology highlights the importance of the augmented quaternion vector in formulating quaternion statistic and the $\mathbb{H}\mathbb{R}$ -calculus. Another example of using the augmented quaternion vector is the minimum mean square error (MMSE) estimator presented in SM-2.

All statistical moments, can be extracted from the derivatives of the AQCF. These moments are in turn useful in the derivation of statistical adaptive processing techniques. However, this requires a robust calculus, a subject of this article. Importantly, the AQCF in (9) establishes a basis for statistical analysis in the quaternion domain. For example, it can be shown that full statistical information of a Gaussian random processes \mathbf{Q} is extractable from its mean $\mathbb{E}\{\mathbf{q}^a\}$ and the augmented covariance $\mathbb{E}\{\mathbf{q}^a \mathbf{q}^{aH}\}$ [17]. For an in-depth treatment of quaternion statistics, the reader is referred to our sister article [21].

Remark 5. Augmenting a quaternion-valued variable with its involution around the ι , \jmath , and κ axes, as formulated in (4), forms the foundations for augmented quaternion statistics and the $\mathbb{H}\mathbb{R}$ -calculus, as it provides a comprehensive method for four dimensional quaternion-valued variables to be considered from four orthogonal rotational perspectives. Although counter intuitive at first, it can be shown that q , q^ι , q^\jmath , q^κ hold different statistical information and can be uncorrelated [15,17]. Specifically regarding the $\mathbb{H}\mathbb{R}$ -calculus, q , q^ι , q^\jmath , and q^κ , must also be considered as algebraically independent [15,19].

II. THE $\mathbb{H}\mathbb{R}$ -CALCULUS

Traditionally, a quaternion-valued function $f(\mathbf{q}) : \mathbb{H}^M \rightarrow \mathbb{H}$ is considered differentiable if and only if it satisfies the Cauchy-Riemann-Fueter condition [19]

$$\frac{\partial f}{\partial q_r} + \iota \frac{\partial f}{\partial q_i} + \jmath \frac{\partial f}{\partial q_j} + \kappa \frac{\partial f}{\partial q_k} = 0 \quad (10)$$

which imposes a severe restriction on admissible functions, as only linear functions can meet this condition [19,22]. The $\mathbb{H}\mathbb{R}$ -calculus [19,22] presents an elegant solution to this problem, where a quaternion function $f(\mathbf{q}) : \mathbb{H}^M \rightarrow \mathbb{H}$ is considered in its augmented formulation as

$$f^a(\mathbf{q}^a) = \left[f(\mathbf{q}^a), f^\iota(\mathbf{q}^a), f^\jmath(\mathbf{q}^a), f^\kappa(\mathbf{q}^a) \right]^\top : \mathbb{H}^{4M} \rightarrow \mathbb{H}^{4M}. \quad (11)$$

Then, the total derivative of $f(\mathbf{q}) = f(\mathbf{q}_r, \mathbf{q}_i, \mathbf{q}_j, \mathbf{q}_k)$ is given by

$$df = d\mathbf{q}_r \frac{\partial f}{\partial \mathbf{q}_r} + d\mathbf{q}_i \frac{\partial f}{\partial \mathbf{q}_i} + d\mathbf{q}_j \frac{\partial f}{\partial \mathbf{q}_j} + d\mathbf{q}_k \frac{\partial f}{\partial \mathbf{q}_k} \quad (12)$$

while, on the other hand, treating $\{\mathbf{q}, \mathbf{q}^\iota, \mathbf{q}^\jmath, \mathbf{q}^\kappa\}$ as a set of “algebraically” independent variables and considering the augmented formulation in (11) yields

$$df = d\mathbf{q} \frac{\partial f}{\partial \mathbf{q}} + d\mathbf{q}^\iota \frac{\partial f}{\partial \mathbf{q}^\iota} + d\mathbf{q}^\jmath \frac{\partial f}{\partial \mathbf{q}^\jmath} + d\mathbf{q}^\kappa \frac{\partial f}{\partial \mathbf{q}^\kappa} \quad (13)$$

for the total derivative of $f(\mathbf{q}^a)$. Now, using (4) in conjunction with (12) and (13) gives the $\mathbb{H}\mathbb{R}$ -derivatives in the form of

$$\begin{bmatrix} \frac{\partial f(\mathbf{q}, \mathbf{q}^\iota, \mathbf{q}^\jmath, \mathbf{q}^\kappa)}{\partial \mathbf{q}} \\ \frac{\partial f(\mathbf{q}, \mathbf{q}^\iota, \mathbf{q}^\jmath, \mathbf{q}^\kappa)}{\partial \mathbf{q}^\iota} \\ \frac{\partial f(\mathbf{q}, \mathbf{q}^\iota, \mathbf{q}^\jmath, \mathbf{q}^\kappa)}{\partial \mathbf{q}^\jmath} \\ \frac{\partial f(\mathbf{q}, \mathbf{q}^\iota, \mathbf{q}^\jmath, \mathbf{q}^\kappa)}{\partial \mathbf{q}^\kappa} \end{bmatrix} = \frac{1}{4} \mathbf{A}^* \begin{bmatrix} \frac{\partial f(\mathbf{q}_r, \mathbf{q}_i, \mathbf{q}_j, \mathbf{q}_k)}{\partial \mathbf{q}_r} \\ \frac{\partial f(\mathbf{q}_r, \mathbf{q}_i, \mathbf{q}_j, \mathbf{q}_k)}{\partial \mathbf{q}_i} \\ \frac{\partial f(\mathbf{q}_r, \mathbf{q}_i, \mathbf{q}_j, \mathbf{q}_k)}{\partial \mathbf{q}_j} \\ \frac{\partial f(\mathbf{q}_r, \mathbf{q}_i, \mathbf{q}_j, \mathbf{q}_k)}{\partial \mathbf{q}_k} \end{bmatrix}. \quad (14)$$

The $\mathbb{H}\mathbb{R}$ -calculus in (14) accommodates the derivation of learning algorithms that reside naturally in the quaternion domain completely bypassing the need to deal with quaternion-valued functions as real-valued vector functions.

From the derivatives of $f(\cdot)$ in (14), of particular interest to information processing applications is the conjugate derivative given by

$$\frac{\partial f}{\partial \mathbf{q}^*} = \frac{1}{4} \left(\frac{\partial f}{\partial \mathbf{q}_r} + \imath \frac{\partial f}{\partial \mathbf{q}_i} + \jmath \frac{\partial f}{\partial \mathbf{q}_j} + \kappa \frac{\partial f}{\partial \mathbf{q}_k} \right) \quad (15)$$

which indicates the direction of maximum rate of change in $f(\cdot)$. Thus, presenting the $\mathbb{H}\mathbb{R}^*$ -derivatives as the gradient operator so that

$$\begin{bmatrix} \frac{\partial f(\mathbf{q}, \mathbf{q}^i, \mathbf{q}^j, \mathbf{q}^k)}{\partial \mathbf{q}^*} \\ \frac{\partial f(\mathbf{q}, \mathbf{q}^i, \mathbf{q}^j, \mathbf{q}^k)}{\partial \mathbf{q}^{i*}} \\ \frac{\partial f(\mathbf{q}, \mathbf{q}^i, \mathbf{q}^j, \mathbf{q}^k)}{\partial \mathbf{q}^{j*}} \\ \frac{\partial f(\mathbf{q}, \mathbf{q}^i, \mathbf{q}^j, \mathbf{q}^k)}{\partial \mathbf{q}^{k*}} \end{bmatrix} = \frac{1}{4} \mathbf{A} \begin{bmatrix} \frac{\partial f(\mathbf{q}_r, \mathbf{q}_i, \mathbf{q}_j, \mathbf{q}_k)}{\partial \mathbf{q}_r} \\ \frac{\partial f(\mathbf{q}_r, \mathbf{q}_i, \mathbf{q}_j, \mathbf{q}_k)}{\partial \mathbf{q}_i} \\ \frac{\partial f(\mathbf{q}_r, \mathbf{q}_i, \mathbf{q}_j, \mathbf{q}_k)}{\partial \mathbf{q}_j} \\ \frac{\partial f(\mathbf{q}_r, \mathbf{q}_i, \mathbf{q}_j, \mathbf{q}_k)}{\partial \mathbf{q}_k} \end{bmatrix} \quad \text{that is } \nabla_{\mathbf{q}^*} f = \frac{1}{4} \mathbf{A} \nabla f. \quad (16)$$

At this point, the formulation of a gradient operator and quaternion derivatives allows us to establish a relation between the AQCF and statistical moments of quaternion random processes, given in SM-3, formulate statistical gradient descent, given in Section III-A, and introduce a quaternion-valued Taylor series expansion, given in Example 2. In what follows, a number rules essential in deriving adaptive processing techniques are presented.

A. Multiplication, Conjugate, and Rotation Rules in the $\mathbb{H}\mathbb{R}$ -Calculus

From (15), it is straightforward to show that [22]

$$\forall \nu \in \mathbb{H} \text{ & } \xi \in \{\imath, \jmath, \kappa\} : \frac{\partial \nu f(\mathbf{q}^a)}{\partial q^\xi} = \nu \frac{\partial f(\mathbf{q}^a)}{\partial q^{\nu^{-1}\xi}} \quad \text{and} \quad \frac{\partial f(\mathbf{q}^a) \nu}{\partial q^\xi} = \frac{\partial f(\mathbf{q}^a)}{\partial q^\xi} \nu. \quad (17)$$

In the same vein, we can formulate the effect of multiplication from both sides, yielding [22]

$$\forall \nu \in \mathbb{H} \wedge \nu^2 = -1 \text{ & } \xi \in \{\imath, \jmath, \kappa\} : \left(\frac{\partial f(\mathbf{q}^a)}{\partial q^\xi} \right)^\nu = \nu \frac{\partial f(\mathbf{q}^a)}{\partial q^\xi} \nu^{-1} = \frac{\partial f^\nu(\mathbf{q}^a)}{\partial q^{\nu\xi}}. \quad (18)$$

Once more, considering (15), we have

$$\left(\frac{\partial f(\mathbf{q}^a)}{\partial \mathbf{q}^*} \right)^* = \frac{1}{4} \left(\frac{\partial f^*(\mathbf{q}^a)}{\partial \mathbf{q}_r} - \frac{\partial f^*(\mathbf{q}^a)}{\partial \mathbf{q}_i} \imath - \frac{\partial f^*(\mathbf{q}^a)}{\partial \mathbf{q}_j} \jmath - \frac{\partial f^*(\mathbf{q}^a)}{\partial \mathbf{q}_k} \kappa \right) = \frac{\partial_{\text{left}} f^*(\mathbf{q}^a)}{\partial \mathbf{q}} \quad (19)$$

where ∂_{left} denotes the placement of partial differential on the left side of the imaginary units $\{\imath, \jmath, \kappa\}$. This can also be seen from (16) which yields $(\nabla_{\mathbf{q}^*} f)^H = \frac{1}{4} (\nabla f)^T \mathbf{A}^H$. These results

can now be used to establish a chain derivative rule in the $\mathbb{H}\mathbb{R}$ -calculus. This is addressed in Section II-B.

Now, consider $\{f(\cdot), g(\cdot)\} : \mathbb{H}^M \rightarrow \mathbb{H}$; then, $h(\mathbf{q}) = f(\mathbf{q})g(\mathbf{q})$ can be expressed in terms of the real-valued components of $f(\cdot)$ and $g(\cdot)$ as

$$h(\mathbf{q}) = (\Re\{f(\mathbf{q})\} + \dots + \kappa \Im_\kappa\{f(\mathbf{q})\})(\Re\{g(\mathbf{q})\} + \dots + \kappa \Im_\kappa\{g(\mathbf{q})\}) \quad (20)$$

with the exact expression given in SM-4. Now, $\forall \xi \in \{1, \iota, \jmath, \kappa\}$, $\frac{\partial h(\mathbf{q})}{\partial \mathbf{q}^\xi}$ can be expressed in terms of its real-valued components, allowing us to use the framework of (10)-(16) in order to formulate the derivative [22]. In this setting, after some tedious mathematical manipulations we arrive at

$$\forall \xi \in \{1, \iota, \jmath, \kappa\} : \begin{cases} \frac{\partial h(\mathbf{q})}{\partial \mathbf{q}^\xi} = f(\mathbf{q}) \frac{\partial g(\mathbf{q})}{\partial \mathbf{q}^{f^*(\mathbf{q})\xi}} + \frac{\partial f(\mathbf{q})}{\partial \mathbf{q}^\xi} g(\mathbf{q}) \\ \frac{\partial h(\mathbf{q})}{\partial \mathbf{q}^{\xi*}} = f(\mathbf{q}) \frac{\partial g(\mathbf{q})}{\partial (\mathbf{q}^{f^*(\mathbf{q})\xi})^*} + \frac{\partial f(\mathbf{q})}{\partial \mathbf{q}^{\xi*}} g(\mathbf{q}). \end{cases} \quad (21)$$

Remark 6. From (19), note that an equivalent calculus can be derived via replacing ∂ with ∂_{left} , see [22]. Although both approaches yield equivalent results, a skilful use of both approaches can simplify derived algorithms, see SM-5.

Example 2. Quaternion-Valued Taylor Series Expansion

Consider the first-order Taylor series expansion in its real-valued formulation given by

$$f(\mathbf{x} + \Delta\mathbf{x}) = f(\mathbf{x}) + (\Delta\mathbf{x})^\top (\nabla_{\mathbf{x}} f(\mathbf{x})) + \mathcal{O}(f(\mathbf{x})) \quad (22)$$

where $\mathbf{x}^\top = [\mathbf{x}_r^\top, \mathbf{x}_i^\top, \mathbf{x}_j^\top, \mathbf{x}_\kappa^\top]$ and $\Delta\mathbf{x}$ represents the change in \mathbf{x} . Now, mapping \mathbf{x} , $\Delta\mathbf{x}$, and $\nabla_{\mathbf{x}} f(\mathbf{x})$ on to the quaternion domain using (29) and (16) allows (22) to be formulated in the quaternion domain as [19]

$$f(\mathbf{x}^a + \Delta\mathbf{x}^a) = f(\mathbf{x}^a) + (\Delta\mathbf{x}^a)^H (\nabla_{\mathbf{x}^a} f(\mathbf{x}^a)) + \mathcal{O}(f(\mathbf{x}^a)).$$

One can formulate higher-order expansion of the series in a similar manner [22].

B. Chain Derivative Rule in the $\mathbb{H}\mathbb{R}$ -Calculus

Consider the quaternion-valued compound function $f(g(\cdot)) : \mathbb{H}^M \rightarrow \mathbb{H}$, where $f(\cdot) : \mathbb{H}^M \rightarrow \mathbb{H}$ and $g(\cdot) : \mathbb{H}^M \rightarrow \mathbb{H}^M$. One can consider the relation between $g^a(\mathbf{q})$ and the

real-valued components of $g(\mathbf{q})$, akin to that given in (4) and (14), yielding

$$\begin{bmatrix} \frac{\partial f(g^a(\mathbf{q}))}{\partial g(\mathbf{q})} \\ \frac{\partial f(g^i(\mathbf{q}))}{\partial g^i(\mathbf{q})} \\ \frac{\partial f(g^j(\mathbf{q}))}{\partial g^j(\mathbf{q})} \\ \frac{\partial f(g^k(\mathbf{q}))}{\partial g^k(\mathbf{q})} \end{bmatrix} = \frac{1}{4} \mathbf{A}^* \begin{bmatrix} \frac{\partial f(g^a(\mathbf{q}))}{\partial g_r(\mathbf{q})} \\ \frac{\partial f(g^a(\mathbf{q}))}{\partial g_i(\mathbf{q})} \\ \frac{\partial f(g^a(\mathbf{q}))}{\partial g_j(\mathbf{q})} \\ \frac{\partial f(g^a(\mathbf{q}))}{\partial g_k(\mathbf{q})} \end{bmatrix} \quad \text{with} \quad \begin{bmatrix} \frac{\partial g_r(\mathbf{q})}{\partial \mathbf{q}} \\ \frac{\partial g_i(\mathbf{q})}{\partial \mathbf{q}} \\ \frac{\partial g_j(\mathbf{q})}{\partial \mathbf{q}} \\ \frac{\partial g_k(\mathbf{q})}{\partial \mathbf{q}} \end{bmatrix} = \frac{1}{4} \mathbf{A}^H \begin{bmatrix} \frac{\partial g(\mathbf{q})}{\partial \mathbf{q}} \\ \frac{\partial g^i(\mathbf{q})}{\partial \mathbf{q}} \\ \frac{\partial g^j(\mathbf{q})}{\partial \mathbf{q}} \\ \frac{\partial g^k(\mathbf{q})}{\partial \mathbf{q}} \end{bmatrix}. \quad (23)$$

Following the framework set in (10)-(16) gives

$$\forall \xi \in \{\iota, j, \kappa\} : \frac{\partial f(g(\mathbf{q}))}{\partial \mathbf{q}^\xi} = \frac{\partial g_r(\mathbf{q})}{\partial \mathbf{q}^\xi} \frac{\partial f(g(\mathbf{q}))}{\partial g_r(\mathbf{q})} + \frac{\partial g_i(\mathbf{q})}{\partial \mathbf{q}^\xi} \frac{\partial f(g(\mathbf{q}))}{\partial g_i(\mathbf{q})} + \frac{\partial g_j(\mathbf{q})}{\partial \mathbf{q}^\xi} \frac{\partial f(g(\mathbf{q}))}{\partial g_j(\mathbf{q})} + \frac{\partial g_k(\mathbf{q})}{\partial \mathbf{q}^\xi} \frac{\partial f(g(\mathbf{q}))}{\partial g_k(\mathbf{q})}. \quad (24)$$

Upon substituting (23) into (24) and using the rotation rule in (18) we arrive at

$$\forall \xi \in \{\iota, j, \kappa\} : \frac{\partial f(g(\mathbf{q}))}{\partial \mathbf{q}^\xi} = \frac{\partial g(\mathbf{q})}{\partial \mathbf{q}^\xi} \frac{\partial f(g(\mathbf{q}))}{\partial g(\mathbf{q})} + \frac{\partial g^\iota(\mathbf{q})}{\partial \mathbf{q}^\xi} \frac{\partial f(g(\mathbf{q}))}{\partial g^\iota(\mathbf{q})} + \frac{\partial g^j(\mathbf{q})}{\partial \mathbf{q}^\xi} \frac{\partial f(g(\mathbf{q}))}{\partial g^j(\mathbf{q})} + \frac{\partial g^\kappa(\mathbf{q})}{\partial \mathbf{q}^\xi} \frac{\partial f(g(\mathbf{q}))}{\partial g^\kappa(\mathbf{q})} \quad (25)$$

with the direction of steepest change given by

$$\frac{\partial f(g(\mathbf{q}))}{\partial \mathbf{q}^*} = \frac{\partial g^*(\mathbf{q})}{\partial \mathbf{q}^*} \frac{\partial f(g(\mathbf{q}))}{\partial g^*(\mathbf{q})} + \frac{\partial g^{\iota*}(\mathbf{q})}{\partial \mathbf{q}^*} \frac{\partial f(g^\iota(\mathbf{q}))}{\partial g^{\iota*}(\mathbf{q})} + \frac{\partial g^{j*}(\mathbf{q})}{\partial \mathbf{q}^*} \frac{\partial f(g^j(\mathbf{q}))}{\partial g^{j*}(\mathbf{q})} + \frac{\partial g^{\kappa*}(\mathbf{q})}{\partial \mathbf{q}^*} \frac{\partial f(g^\kappa(\mathbf{q}))}{\partial g^{\kappa*}(\mathbf{q})}. \quad (26)$$

Most useful in adaptive information processing applications is the case where $g(\cdot) : \mathbb{H}^M \rightarrow \mathbb{R}$ and $f(\cdot) : \mathbb{R} \rightarrow \mathbb{R}$. In this case, from (24)-(26), we have

$$\forall \xi \in \{\iota, j, \kappa\} : \frac{\partial f(g(\mathbf{q}))}{\partial \mathbf{q}^\xi} = \frac{\partial g(\mathbf{q})}{\partial \mathbf{q}^\xi} \frac{\partial f(g(\mathbf{q}))}{\partial g(\mathbf{q})} \text{ and } \frac{\partial f(g(\mathbf{q}))}{\partial \mathbf{q}^{\xi*}} = \frac{\partial g(\mathbf{q})}{\partial \mathbf{q}^{\xi*}} \frac{\partial f(g(\mathbf{q}))}{\partial g(\mathbf{q})}. \quad (27)$$

The chain derivative rule allows for the derivation of quaternion-valued adaptive learning techniques. The case of linear (*cf.* nonlinear) adaptive filters is presented in SM-5 (*cf.* SM-6), while its application in quaternion-valued backpropagation demonstrated in Section III-C.

III. LEARNING AND DECISION MAKING IN THE QUATERNION DOMAIN

A. Statistical Gradient Descent

Consider the problem of tracking the state of an evolving system, whether a physical system (aircraft) or state of adaptive processing machinery (weights of a quaternion-valued neural network). The state of this system is represented via the state vector sequence $\{\mathbf{x}_{[n]} : n \in \mathbb{N}\}$ so that

$$\mathbf{x}_{[n+1]} = f(\mathbf{x}_{[n]}, \mathbf{v}_{[n]}, \mathbf{u}_{[n]}) \quad (28)$$

where $f(\cdot)$, $\mathbf{u}_{[n]}$, and $\mathbf{v}_{[n]}$, are the evolution function, a known control input, and a noise vector at time instant n . Informative observations regarding the state vector are assumed available through observations

$$\mathbf{y}_{[n]} = h(\mathbf{x}_{[n]}, \mathbf{w}_{[n]}) \quad (29)$$

where $h(\cdot)$ denotes the observation function, while $\mathbf{y}_{[n]}$ and $\mathbf{w}_{[n]}$ are the observation and observation noise at time instant n . The aim is to find the estimate of $\mathbf{x}_{[n]}$ given the available information set $\mathcal{I}_{[n]} = \{\mathbf{u}_{[1:n]}, \mathbf{y}_{[1:n]}\}$, formulated as $\hat{\mathbf{x}}_{[n]} = E\{\mathbf{x}_{[n]} | \mathcal{I}_{[n]}\}$.

From (9) and using (15), we have

$$\hat{\mathbf{x}}_{[n]}^a = \frac{4}{\xi} \frac{\partial \Phi_{\mathbf{x}_{[n]}^a | \mathcal{I}_{[n]}}(\mathbf{s}^a)}{\partial \mathbf{s}^{a*}} \Big|_{\mathbf{s}=\mathbf{0}} = E\{\mathbf{x}_{[n]}^a | \mathcal{I}_{[n]}\}.$$

In the same vain, the *a priori* estimate is defined as

$$\psi_{[n+1]}^a = \frac{4}{\xi} \frac{\partial \Phi_{\mathbf{x}_{[n+1]}^a | \mathcal{I}_{[n]}}(\mathbf{s}^a)}{\partial \mathbf{s}^{a*}} \Big|_{\mathbf{s}=\mathbf{0}} = E\{\mathbf{x}_{[n+1]}^a | \mathcal{I}_{[n]}\}. \quad (30)$$

where using (28) yields

$$\Phi_{\mathbf{x}_{[n+1]}^a | \mathcal{I}_{[n]}}(\mathbf{s}^a) = E\left\{e^{\frac{\xi}{4}\mathbf{s}^{aH}\mathbf{x}_{[n+1]}^a} | \mathcal{I}_{[n]}\right\} = E\left\{e^{\frac{\xi}{4}\mathbf{s}^{aH}f^a(\mathbf{x}_{[n]}, \mathbf{v}_{[n]}, \mathbf{u}_{[n]})} | \mathbf{y}_{[1:n]}\right\}. \quad (31)$$

A substitution of (30) into (31) gives

$$\psi_{[n+1]}^a = E\{f^a(\mathbf{x}_{[n]}, \mathbf{v}_{[n]}, \mathbf{u}_{[n]}) | \mathbf{y}_{[1:n]}\} \approx E\{f^a(\mathbf{x}_{[n]}, \mathbf{u}_{[n]}) | \mathbf{y}_{[1:n]}\} \quad (32)$$

allowing for an approximation of $\psi_{[n+1]}^a$ to be formulated as

$$\psi_{[n+1]}^a \approx E\left\{\mathbf{A}_{[n]}\hat{\mathbf{x}}_{[n]}^a + \mathcal{O}_{f(\mathbf{x}_{[n]}, \mathbf{u}_{[n]})} | \mathbf{y}_{[1:n]}\right\} \approx \mathbf{A}_{[n]}\hat{\mathbf{x}}_{[n]}^a + E\{\mathcal{O}_{f(\mathbf{x}_{[n]}, \mathbf{u}_{[n]})} | \mathbf{y}_{[1:n]}\} \quad (33)$$

where $\mathbf{A}_{[n]}$ represents the linearisation of $f(\cdot)$ at $\{\hat{\mathbf{x}}_{[n]}^a, \mathbf{u}_{[n]}^a\}$ obtainable through the gradient operator (16). In addition, we have

$$\hat{\mathbf{x}}_{[n+1]}^a = \frac{4}{\xi} \frac{\partial \Phi_{\mathbf{x}_{[n+1]}^a | \mathcal{I}_{[n+1]}}(\mathbf{s})}{\partial \mathbf{s}^{a*}}$$

with $\Phi_{\mathbf{x}_{[n+1]}^a | \mathcal{I}_{[n+1]}}(\mathbf{s}) = E\left\{e^{\frac{\xi}{4}\mathbf{s}^{aH}f^a(\mathbf{x}_{[n]}, \mathbf{u}_{[n]})} e^{\frac{\xi}{4}\mathbf{s}^{aH}\mathcal{O}_{(f(\mathbf{x}_{[n]}, \mathbf{v}_{[n]}, \mathbf{u}_{[n]}))}} | \mathbf{y}_{[1:n+1]}\right\}$.

Assuming that dependency of $\mathcal{O}_{(f(\mathbf{x}_{[n]}, \mathbf{v}_{[n]}, \mathbf{u}_{[n]}))}$ on $f(\mathbf{x}_{[n]}, \mathbf{u}_{[n]})$ is negligible, (33) can be reformulated to give

$$\Phi_{\mathbf{x}_{[n+1]}^a | \mathcal{I}_{[n+1]}}(\mathbf{s}^a) = \Phi_{\mathbf{x}_{[n+1]}^a | \mathcal{I}_{[n]}}(\mathbf{s}^a) E\left\{e^{\frac{\xi}{4}\mathbf{s}^{aH}\mathcal{O}_{(f(\mathbf{x}_{[n]}, \mathbf{v}_{[n]}, \mathbf{u}_{[n]}))}} | \mathbf{y}_{[n+1]}\right\}$$

where $\Phi_{\mathbf{x}_{[n+1]}^a | \mathcal{I}_{[n+1]}}(\mathbf{s}^a)$ consists of two parts, one representing the *a priori*, $\Phi_{\mathbf{x}_{[n+1]}^a | \mathcal{I}_{[n]}}(\mathbf{s}^a)$, and the other, representing the *a posteriori*, $\mathbb{E} \left\{ e^{j\mathbf{s}^T \mathcal{O}_{(\mathbf{f}_{[n]}(\mathbf{x}_{[n]}, \mathbf{v}_{[n]}, \mathbf{u}_{[n]}))}} | \mathbf{y}_{[n+1]} \right\}$, correction. Moreover, from (32), we have

$$\hat{\mathbf{x}}_{[n+1]}^a = \psi_{[n+1]}^a + \mathbb{E} \left\{ \mathcal{O}_{(\mathbf{f}_{[n]}(\mathbf{x}_{[n]}, \mathbf{v}_{[n]}, \mathbf{u}_{[n]}))} | \mathbf{y}_{[n+1]} \right\}. \quad (34)$$

Although the estimate, $\hat{\mathbf{x}}_{[n+1]}^a$, in (34) can be approximated using particle based inference techniques, the $\mathbb{H}\mathbb{R}$ -calculus can provide a more computationally friendly and mathematically tractable solutions. From (28) and (29), the following error terms are defined

$$\boldsymbol{\epsilon}_{[n]} = \mathbf{x}_{[n]} - \hat{\mathbf{x}}_{[n]} \quad \text{and} \quad \tilde{\boldsymbol{\epsilon}}_{[n]} = \mathbf{y}_{[n]} - \hat{\mathbf{y}}_{[n]} \quad (35)$$

where $\hat{\mathbf{y}}_{[n+1]} = h(\psi_{[n+1]})$ is projection of $\psi_{[n+1]}$ onto the observation space. Now, let $d(\cdot)$ be a quaternion-valued metric function. Then, $\{\boldsymbol{\epsilon}_{[n]} : n \in \mathbb{N}\}$ being exponentially stable sequence implies that $\{\tilde{\boldsymbol{\epsilon}}_{[n]} : n \in \mathbb{N}\}$ should also be exponentially stable.² In this setting, $\nabla_{\psi_{[n+1]}^{a*}} d(\tilde{\boldsymbol{\epsilon}}_{[n+1]})$ indicates a direction of ascent for $d(\tilde{\boldsymbol{\epsilon}}_{[n+1]})$, and hence, an adaptive filtering structure is formulated as

$$\hat{\mathbf{x}}_{[n+1]}^a \approx \psi_{[n+1]}^a - \mathbf{G}_{[n]} \mathbb{E} \left\{ \nabla_{\psi_{[n+1]}^{a*}} d(\tilde{\boldsymbol{\epsilon}}_{[n+1]}) \right\} \approx \psi_{[n+1]}^a - \mathbf{G}_{[n]} \nabla_{\psi_{[n+1]}^{a*}} d(\tilde{\boldsymbol{\epsilon}}_{[n+1]}) \quad (36)$$

where $\{\mathbf{G}_{[n]} : n \in \mathbb{N}\}$ is a gain sequence while $\mathbb{E} \left\{ \nabla_{\psi_{[n+1]}^{a*}} d(\tilde{\boldsymbol{\epsilon}}_{[n+1]}) \right\}$ is replaced with its instantaneous value, $\nabla_{\psi_{[n+1]}^{a*}} d(\tilde{\boldsymbol{\epsilon}}_{[n+1]})$, as in most cases these expectations are not available.

Remark 7. Most adaptive filtering techniques can be formalised within the framework derived in this section. As an example, the stochastic gradient descent technique is used to derive the quaternion-valued Kalman filter in Example 3.

B. Sensor Fusion

Consider the set of sensors $\{S_l : l = 1, \dots, M\}$, where each sensor, S_l , has estimate $\hat{\mathbf{x}}_{l,[n]} = \mathbb{E} \left\{ \mathbf{x}_{[n]} | \mathbf{y}_{l,[1:n]} \right\}$ with $\mathbf{y}_{l,[1:n]}$ repressing the observation of sensor l up to time instant n . The aim is to find $\hat{\mathbf{x}}_{[n]} = \mathbb{E} \left\{ \mathbf{x}_{[n]} | \hat{\mathbf{x}}_{1:M,[1:n]} \right\}$. This is *on par* with the problem considered in Section III-A so that; i) $\{f(\cdot), h(\cdot)\}$ become identity functions, ii) $\psi_{[n]}$ becomes a vector incorporating any *a priori* information, and iii) $\begin{bmatrix} \hat{\mathbf{x}}_{1,[n]}^{a\top} & \dots & \hat{\mathbf{x}}_{m,[n]}^{a\top} \end{bmatrix}^\top$ becomes the available

²Note that; i) converse of the statement might not hold true, and ii) the statement implicitly implies that $h(\cdot)$ and $f(\cdot)$ are bounded.

observation at time instant n , i.e., $\mathbf{y}_{[n]}$. Using the the same machinery as in Section III-A, from (36) it follows that

$$\hat{\mathbf{x}}_{[n+1]}^a = \psi_{[n+1]}^a - \mathbf{G}_{[n]} \nabla_{\psi_{[n+1]}^a} d \left(\psi_{[n+1]}^a - \mathbf{y}_{[n]}^a \right). \quad (42)$$

Furthermore, it is generally assumed that; i) sensor estimates are independent with Gaussian distributions, ii) $d(\cdot) = \|\cdot\|^2$. Thus, through the framework presented in Example 3, (42) simplifies into

$$\hat{\mathbf{x}}_{[n+1]}^a = \psi_{[n+1]}^a - \mathbf{G}_{[n]} \left(\sum_{l=1}^M \boldsymbol{\Sigma}_{(\mathbf{x}_{[n]}^a - \hat{\mathbf{x}}_{l,[n]}^a)}^{-1} \hat{\mathbf{x}}_{l,[n]}^a \right) \quad (43)$$

where $\boldsymbol{\Sigma}_{(\mathbf{x}_{[n]}^a - \hat{\mathbf{x}}_{l,[n]}^a)} = \mathbb{E} \left\{ \left(\mathbf{x}_{[n]}^a - \hat{\mathbf{x}}_{l,[n]}^a \right) \left(\mathbf{x}_{[n]}^a - \hat{\mathbf{x}}_{l,[n]}^a \right)^H \right\}$ and $\mathbf{G}_{[n]}$ is selected to minimise $\boldsymbol{\Sigma}_{(\mathbf{x}_{[n]}^a - \hat{\mathbf{x}}_{l,[n]}^a)}$. Although the required augmented covariance matrices, $\{\boldsymbol{\Sigma}_{(\mathbf{x}_{[n]}^a - \hat{\mathbf{x}}_{l,[n]}^a)} : l = 1, \dots, M\}$, are tractable in some cases (see Example 3), it is generally assumed that $\psi_{[n+1]}^a \rightarrow 0$ and $\forall l : \boldsymbol{\Sigma}_{(\mathbf{x}_{[n]}^a - \hat{\mathbf{x}}_{l,[n]}^a)} \rightarrow w_l \mathbf{I}$, further simplifying (43) into

$$\mathbf{x}_{[n+1]}^a = \sum_{n=1}^M w_l \mathbf{x}_{l,[n]}^a \quad (44)$$

where we have assumed $\sum_{l=1}^M w_l = 1$ to enforce³ $\mathbf{G}_{[n]} \rightarrow \mathbf{I}$. Application of sensor fusion in distributed estimation and federated learning is elaborated upon in SM-7.

C. Backpropagation in the Quaternion Domain

Consider a neural network of L layers with N_l neurons in the l th layer. Output of the n th neuron on the l th layer can be formulated as

$$y_{l,n} = \sum_{m=1}^{N_l} w_{l,n,m} x_{l-1,m} + b_{l,n}$$

where $w_{l,n,m}$ are quaternion-valued weights and $b_{l,n}$ is the bias term, while

$$x_{l,n} = f(y_{l,n})$$

is the output of neuron n in layer l with $f(\cdot)$ represents a nonlinear quaternion-valued activation function. The aim is to find the gradient of the cost function

$$J = \frac{1}{2} \sum_{m=1}^{N_L} \|d_m - x_{L,m}\|^2 \quad (45)$$

³Note that since the combination weight w_l is taking the role of a positive definite covariance; then, $w_l \in \mathbb{R}^+$.

with respect to the quaternion-valued weights, where d_m denoting a desired output. Given the cost function J in (45), the gradient is given by

$$\nabla_{\mathbf{W}_L^*} J = -\frac{1}{2} \sum_{\forall \zeta \in \{1, i, j, k\}} \left(\nabla_{\mathbf{W}_L^\zeta} J^H \boldsymbol{\epsilon} \right)^\zeta$$

with

$$\mathbf{W}_L = \begin{bmatrix} w_{L,1,1} & \dots & w_{L,1,N_{L-1}} \\ \vdots & \ddots & \vdots \\ w_{L,N_L,1} & \dots & w_{L,N_L,N_{L-1}} \end{bmatrix} \quad \text{and} \quad \boldsymbol{\epsilon} = \begin{bmatrix} d_1 \\ \dots \\ d_{N_L} \end{bmatrix} - \underbrace{\begin{bmatrix} x_{L,1} \\ \dots \\ x_{L,N_L} \end{bmatrix}}_{\mathbf{x}_L}.$$

This gradient can be described in a layer-by-layer manner so that

$$\boldsymbol{\delta}_l = \begin{cases} \boldsymbol{\epsilon} & l = L \\ (\mathbf{W}_{l+1} \mathbf{x}_{l+1})^H \boldsymbol{\delta}_{l+1} & l \neq L. \end{cases}$$

The weight and bias update rules for the output layer then become

$$\mathbf{W}_L \leftarrow \mathbf{W}_L + \gamma \boldsymbol{\delta}_L \mathbf{x}_{L-1}^H \quad \text{and} \quad \begin{bmatrix} b_{L,1} & \vdots & b_{L,N_L} \end{bmatrix}^T \leftarrow \begin{bmatrix} b_{L,1} & \vdots & b_{L,N_L} \end{bmatrix}^T + \gamma \boldsymbol{\delta}_L$$

while the weight and bias update rules for the hidden layers are given by

$$\mathbf{W}_l \leftarrow \mathbf{W}_l + \gamma \sum_{\forall \zeta \in \{1, i, j, k\}} (\boldsymbol{\delta}_l)^\zeta \mathbf{x}_{l-1}^H \quad \text{and} \quad \begin{bmatrix} b_{l,1} \\ \vdots \\ b_{l,N_l} \end{bmatrix} \leftarrow \begin{bmatrix} b_{l,1} \\ \vdots \\ b_{l,N_l} \end{bmatrix} + \gamma \sum_{\forall \zeta \in \{1, i, j, k\}} (\boldsymbol{\delta}_l)^\zeta$$

where $\gamma \in \mathbb{R}^+$ is the learning rate.

D. Linear Dynamic Programming and Initial Elements of Reinforcement Learning

To revisit the fundamental problem at the heart of reinforcement learning [24] and control [20] applications, consider the optimisation problem formulated as:

$$\text{minimise} : J = \mathbf{x}_{[N]}^{aH} \mathbf{T}^a \mathbf{x}_{[N]}^a + \sum_{n=1}^{N-1} \left(\mathbf{x}_{[n]}^{aH} \mathbf{Q} \mathbf{x}_{[n]}^a + \mathbf{u}_{[n]}^{aH} \mathbf{R} \mathbf{u}_{[n]}^a \right) \quad (46)$$

$$\text{so that: } \mathbf{u}_{[n]} = \mathbf{G}_{[n]} \mathbf{x}_n^a \quad \text{and} \quad \mathbf{x}_{[n+1]}^a = \mathbf{A} \mathbf{x}_n^a + \mathbf{B} \mathbf{u}_{[n]}^a \quad (47)$$

where N represents the time horizon for calculation of inputs $\{\mathbf{u}_{[n]} : n \in \mathbb{N}\}$, matrices $\{\mathbf{T}, \mathbf{R}, \mathbf{Q}\}$ are Hermitian transpose symmetric and positive semi-definite, that is, $\forall \mathbf{z} \in \mathbb{H} \quad \mathbf{z}^H \mathbf{M} \mathbf{z} \geq 0$, while $\mathbf{G}_{[n]}$ is the feedback gain matrix (optimal policy).

The matrices \mathbf{T} , \mathbf{Q} , and \mathbf{R} penalise the final deviation from the desired state, deviation from the desisted state during the process, and implementation of an input.

The goal of the problem is to find the optimal feedback gain matrix at each time instant. To this end, the cost function in (46) is sectioned into time specific cost functions given by

$$J_{[n]} = \begin{cases} \mathbf{x}_{[N]}^{a\mathsf{H}} \mathbf{T} \mathbf{x}_{[N]}^a & \text{if } n = N, \\ \mathbf{x}_{[n]}^{a\mathsf{H}} \mathbf{Q} \mathbf{x}_{[n]}^a + \mathbf{u}_{[n]}^{a\mathsf{H}} \mathbf{R} \mathbf{u}_{[n]}^a & \text{otherwise.} \end{cases} \quad (48)$$

Now, upon inserting (47) into (48) we have

$$J_{[n]} = \mathbf{x}_{[n]}^{a\mathsf{H}} \mathbf{Q} \mathbf{x}_{[n]}^a + \mathbf{u}_{[n]}^{a\mathsf{H}} \mathbf{R} \mathbf{u}_{[n]}^a = \mathbf{x}_{[n]}^{a\mathsf{H}} \Psi_{[n]} \mathbf{x}_{[n]}^a \quad (49)$$

with $\Psi_{[n]} = \mathbf{Q} + \mathbf{G}_{[n]}^{\mathsf{H}} \mathbf{R} \mathbf{G}_{[n]}$. The expressions in (48) and (49) allow the time accumulative cost function to be defined as

$$\mathcal{J}_{[n]} = \sum_{m=n}^N J_{[m]}. \quad (50)$$

This indicates that there exists a positive definite Hermitian symmetric matrix $\mathbf{P}_{[n]}$, the existence of which is proven in SM-8, such that

$$\mathcal{J}_{[n]} = \mathbf{x}_{[n]}^{a\mathsf{H}} \mathbf{P}_{[n]} \mathbf{x}_{[n]}^a \quad (51)$$

which extends the Hamilton-Jacobi-Bellman (see [20]) for solving quaternion-valued optimisation problems.

Moving backwards in time with the implicit assumption that inputs for future time instances have been obtained, the task becomes that of calculating the input at the previous time instant resulting in⁴

$$2\mathcal{J}_{[n]} = \min_{\mathbf{u}_{[n]}} \left\{ 2\mathbf{x}_{[n]}^{a\mathsf{H}} \mathbf{Q} \mathbf{x}_{[n]}^a + 2\mathbf{u}_{[n]}^{a\mathsf{H}} \mathbf{R} \mathbf{u}_{[n]} + 2\mathcal{J}_{[n]} \right\}. \quad (52)$$

The minimum of (52) occurs at

$$\mathbf{u}_{[n]} = - \left(\mathbf{R} + \mathbf{B}^{\mathsf{H}} \mathbf{P}_{[n+1]} \mathbf{B} \right)^{-1} \mathbf{B}^{\mathsf{H}} \mathbf{P}_{[n+1]} \mathbf{A}^a \mathbf{x}_{[n]}^a. \quad (53)$$

Thus, from (53) and (47) it becomes clear that $\mathbf{G}_{[n]} = - \left(\mathbf{R} + \mathbf{B}^{\mathsf{H}} \mathbf{P}_{[n+1]} \mathbf{B} \right)^{-1} \mathbf{B}^{\mathsf{H}} \mathbf{P}_{[n+1]} \mathbf{A}$. Crucially, replacing (53) into (52) and after some mathematical manipulation, we have

$$\mathbf{S}_{[n]} = \left(\left(\mathbf{A}^{\mathsf{H}} \mathbf{S}_{[n+1]} \mathbf{A} + \mathbf{Q} \right)^{-1} + \mathbf{B} \mathbf{R}^{-1} \mathbf{B}^{\mathsf{H}} \right)^{-1} \quad (54)$$

⁴All elements in (52) have been scaled by a factor of 2 in order to compensate for the scales generated after differentiation.

where $\mathbf{P}_{[n]} = \mathbf{A}^H \mathbf{S}_{[n+1]} \mathbf{A} + \mathbf{Q}$. Note that (54) is a quaternion-valued algebraic Riccati recursion, see SM-1, that converges to a unique solution as $n \rightarrow \infty$ given $\{\mathbf{A}^H, \mathbf{Q}^{\frac{1}{2}}\}$ (cf. $\{\mathbf{A}, \mathbf{B}^H\}$) are stabilisable (cf. detectable), see Example 3 and [15,23]. Finally, the inputs can be formulated as

$$\mathbf{u}_{[n]} = -\mathbf{R}^{-1} \mathbf{B}^H \mathbf{S}_{[n+1]} \mathbf{A} \mathbf{x}_{[n]}^a. \quad (55)$$

IV. CONCLUSION

The article has revisited the $\mathbb{H}\mathbb{R}$ -calculus and its application in processing quaternion-valued signals. The main tools in this area, such as the chain derivative rule and the multiplication derivative rule, have been derived in a straightforward manner. These rules have been in turn used to derive a stochastic gradient descent algorithm that forms the basis for adaptive filtering techniques in the quaternion domain. For rigour, application of the $\mathbb{H}\mathbb{R}$ -calculus in Kalman filtering and quaternion-valued linear dynamic programming have also been explored. This enables the use of quaternions in statistical learning and decision making applications, a number of which are presented in the supplementary material accompanying the manuscript.

REFERENCES

- [1] J. Voight, *Quaternion Algebras*, Springer, 2021.
- [2] T. L. Hankins, “Triplets and triads: Sir William Rowan Hamilton on the metaphysics of mathematics,” *Isis*, vol. 68, no. 2, pp. 175–193, 1977.
- [3] D. Finkelstein, J. M. Jauch, S. Schiminovich, and D. Speiser, “Foundations of Quaternion Quantum Mechanics,” *Journal of Mathematical Physics*, vol. 3, no. 2, pp. 207–220, December 2004.
- [4] M. Danielewski and S. Lucjan, “Foundations of the quaternion quantum mechanics,” *Entropy*, vol. 22, no. 12, 2020.
- [5] J. C. Maxwell, *A Treatise on Electricity and Magnetism*, Dover Publications, New York, 1873, ISBN 0-486-60636-8 (Vol. 1) and 0-486-60637-6 (Vol. 2).
- [6] S. P. Talebi and Danilo P. Mandic, “A quaternion frequency estimator for three-phase power systems,” *In Proceedings of IEEE International Conference on Acoustics, Speech and Signal Processing*, pp. 3956–3960, 2015.
- [7] S. P. Talebi, S. Kanna, and D. P. Mandic, “A distributed quaternion Kalman filter with applications to smart grid and target tracking,” *IEEE Transactions on Signal and Information Processing over Networks*, vol. 2, no. 4, pp. 477–488, December 2016.
- [8] F. A. Tobar and D. P. Mandic, “Quaternion reproducing kernel Hilbert spaces: Existence and uniqueness conditions,” *IEEE Transactions on Information Theory*, vol. 60, no. 9, pp. 5736–5749, 2014.
- [9] D. Comminiello, M. Lella, S. Scardapane, and A. Uncini, “Quaternion convolutional neural networks for detection and localization of 3D sound events,” *In Proceedings of IEEE International Conference on Acoustics, Speech and Signal Processing*, pp. 8533–8537, 2019.

- [10] S. Miron, N. Le Bihan, and J. I. Mars, “Quaternion-MUSIC for vector-sensor array processing,” *IEEE Transactions on Signal Processing*, vol. 54, no. 4, pp. 1218–1229, April 2006.
- [11] T. A. Ell and S. J. Sangwine, “Hypercomplex Fourier transforms of color images,” *IEEE Transactions on Image Processing*, vol. 16, no. 1, pp. 22–35, January 2007.
- [12] S. Stern and R. F. H. Fischer, “Quaternion-valued multi-user MIMO transmission via dual-polarized antennas and QLLL reduction,” *In Proceedings of International Conference on Telecommunications*, pp. 63–69, 2018.
- [13] J. Seberry, K. Finlayson, S. S. Adams, T. A. Wysocki, T. Xia, and B. J. Wysocki, “The theory of quaternion orthogonal designs,” *IEEE Transactions on Signal Processing*, vol. 56, no. 1, pp. 256–265, january 2008.
- [14] V. Kliuchnikov and J. T. Yard, “A framework for exact synthesis,” Tech. Rep., 2015, arXiv preprint arXiv:1504.04350.
- [15] S. P. Talebi, *Adaptive filtering algorithms for quaternion-valued signals*, Ph.D. thesis, Imperial College London, 2016.
- [16] T. A. Ell and S. J. Sangwine, “Quaternion involutions and anti-involutions,” *Computers & Mathematics with Applications*, vol. 53, no. 1, pp. 137–143, 2007.
- [17] C. C. Took and D. P. Mandic, “Augmented second-order statistics of quaternion random signals,” *Signal Processing*, vol. 91, no. 2, pp. 214–224, 2011.
- [18] D. P. Mandic, C. Jahanchahi, and C. C. Took, “A quaternion gradient operator and its applications,” *IEEE Signal Processing Letters*, vol. 18, no. 1, pp. 47–50, January 2011.
- [19] C. Jahanchahi, *Quaternion valued adaptive signal processing*, Ph.D. thesis, Imperial College London, 2013.
- [20] R. F. Stengel, *Optimal Estimation and Control*, Dover Publications, 1994.
- [21] C. Cheong Took, S. P. Talebi, R. M. Fernandez Alcala, and D. P. Mandic, “Augmented statistics of quaternion random variables: A lynchpin of quaternion learning machines,” *IEEE Signal Processing Magazine*, Submitted.
- [22] D. Xu D, C. Jahanchahi, C. C. Took, and D. P. Mandic, “Enabling quaternion derivatives: The generalized HR calculus,” *Royal Society Open Science*, vol. 2, no. 8, August 2015.
- [23] S. P. Talebi, S. Werner, and D. P. Mandic, “Quaternion-valued distributed filtering and control,” *IEEE Transactions on Automatic Control*, vol. 65, no. 10, pp. 4246–4257, 2020.
- [24] Richard S. Sutton and Andrew G. Barto, *Reinforcement Learning: An Introduction*, MIT Press, second edition, 2018.
- [25] D. Alfsmann, H. G. Gockler, S. J. Sangwine, and T. A. Ell, “Hypercomplex algebras in digital signal processing: Benefits and drawbacks,” *In Proceedings of European Signal Processing Conference*, pp. 1322–1326, September 2007.
- [26] V. P. Brasil, A. L. F. Filho, and J. Y. Ishihara, “Electrical three phase circuit analysis using quaternions,” *International Conference on Harmonics and Quality of Power*, pp. 1–6, 2018.
- [27] O. V. Nos, “The quaternion model of doubly-fed induction motor,” *International Forum on Strategic Technology*, pp. 32–36, 2016.
- [28] J. L. Crassidis, F. L. Markley, and Y. Cheng, “Survey of nonlinear attitude estimation methods,” *Journal of Guidance, Control, and Dynamics*, vol. 30, no. 1, pp. 12–28, January 2007.

Danilo Mandic (d.mandic@ic.ac.uk) received the Ph.D. degree in nonlinear adaptive signal processing in 1999 from Imperial College, London, where he is now a Professor. He specialises in Statistical Learning Theory, Machine Intelligence, and Statistical Signal Processing. Recently, he was invited as a distinguished lecturer by

the IEEE Signal Processing Society to talk on a wide range of topics ranging from graph theory to innovation in education.

Sayed Pouria Talebi (s.talebi12@alumni.imperial.ac.uk) received his doctorate degree from Imperial College London, where his research focused on quaternion-valued signal processing. He has served as a researcher at a number of institutions including University of Cambridge. He is currently a lecturer at University of Roehampton. Some of his contributions to this area include formulation of the theory of quaternion-valued multi-agent systems, formulation of the basis of quaternion-valued control theory, and quaternion-valued nonlinear/non-Gaussian signal processing. In his work, he has demonstrated the usefulness of quaternions for modelling power distributions systems and passive target tracking.

Clive Cheong Took (clive.cheongtook@rhul.ac.uk) received his doctorate from Cardiff University. He is a senior lecturer at Royal Holloway, University of London, U.K. He has been working on quaternion signal processing since 2008 and delivered a tutorial on this topic in the conference EUSIPCO 2011. Some of his contributions to this area include augmented statistics, adaptive learning, and novel matrix factorisations. Over the years, Clive has demonstrated the usefulness of quaternions to address various problems such as source separation, prediction or estimation, and classification for various biomedical applications. Recently, his research in quaternions has nurtured his interest in three-dimensional rotations for which quaternions are popular for. He is a Senior Member of IEEE.

Yili Xia (yili_xia@seu.edu.cn) received the Ph.D. degree in adaptive signal processing from Imperial College London in 2011. Since 2013, he has been an Associate Professor in signal processing with the School of Information Science and Engineering, Southeast University, where he is currently the Deputy Head of the Department of Information and Signal Processing Engineering. His research interests include complex and hyper-complex statistical analysis. He was a recipient of the Best Student Paper Award at the International Symposium on Neural Networks (ISNN) in 2010 (coauthor) and the Education Innovation Award at the IEEE International Conference on Acoustics, Speech, and Signal Processing (ICASSP) in 2019. He is an Associate Editor for the IEEE Transactions on Signal Processing.

Dongpo Xu (dongpoxu@gmail.com) received the Ph.D. degree in computational mathematics from the Dalian University of Technology, Dalian, China in 2009. He was a Lecturer with the College of Science, Harbin Engineering University and a Visiting Scholar with the Department of Electrical and Electronic Engineering, Imperial College London. He is currently a Professor with the School of Mathematics and Statistics, Northeast Normal University, Changchun, China. His current research interests include neural networks, machine learning, and signal processing. Dr. Xu has been an Associate Editor of the Frontiers in Artificial Intelligence and the Frontiers in Big Data.

Min Xiang (xiang_min@buaa.edu.cn) received the Ph.D. degree in electrical engineering from Imperial College London, London, U.K., in 2018. He was a Research Associate with Imperial College London from 2018 to 2020. Since 2020, he has been an Associate Professor with Beihang University, Beijing, China. His research interests include statistical signal processing, specifically quaternion-valued signal processing.

Pauline Bourigault (p.bourigault22@imperial.ac.uk) is currently pursuing her doctoral degree in AI and Machine Learning enrolled in the UKRI Centre for Doctoral Training in AI for Healthcare at Imperial College London. Her current research focuses on 3D human pose estimation.

SUPPLEMENTARY MATERIAL

SM-1: Quaternion Rotations and Algebraic Lyapunov/Riccati Recursions

Consider the evolution of a quaternion-valued sequence $\{q_{[n]} : n \in \mathbb{N}\}$ that encapsulates all three transformations (rotation, scaling, and shift) of a real-world systems operating in the three-dimensional space, e.g., robot arm, aircraft/vehicle, or an particle. Based on the quaternion model of rotation given in (6), the evolutions of $q_{[n]}$ are formulated as

$$q_{[n+1]} = a_{[n]} \mu_{[n]} q_{[n]} \mu_{[n]}^{-1} + q_{\text{shift}_{[n]}} = \sqrt{a_{[n]}} \mu_{[n]} q_{[n]} \sqrt{a_{[n]}} \mu_{[n]}^{-1} + q_{\text{shift}_{[n]}} \quad (56)$$

where $a_{[n]} \in \mathbb{R}$ and $q_{\text{shift}_{[n]}}$ represent the scaling and shift factors. Moreover, as an associative hypercomplex algebra, quaternions have an isomorphic matrix algebra [25], so that

$$\forall q \in \mathbb{H} \leftrightarrow \mathbf{Q} = \begin{bmatrix} q_r & -q_i & -q_j & q_k \\ q_i & q_r & -q_k & -q_j \\ q_j & q_k & q_r & q_i \\ -q_k & q_j & -q_i & q_r \end{bmatrix} \in \mathbb{R}^4 \times \mathbb{R}^4 \quad (57)$$

where \mathbf{Q} is the representation of q in the isomorphic matrix algebra [25]. Thus, using the duality in (57) the expression in (56) can be transformed into the real-valued Lyapunov style recursion

$$\mathbf{Q}_{[n+1]} = \mathbf{M}_{[n]} \mathbf{Q}_{[n+1]} \mathbf{M}_{[n]}^H + \mathbf{Q}_{\text{shift}_{[n]}}$$

with $\mathbf{Q}_{[n]}$, $\mathbf{M}_{[n]}$, and $\mathbf{Q}_{\text{shift}_{[n]}}$ representing the real-valued matrix duals of $q_{[n]}$, $\sqrt{a} \mu$, and $q_{\text{shift}_{[n]}}$. In addition, consider the Riccati recursions in its information matrix formulation given as

$$\mathbf{Q}_{[n+1]} = \underbrace{\left(\underbrace{\left(\mathbf{M}_{[n]} \mathbf{Q}_{[n]} \mathbf{M}_{[n]}^H + \mathbf{Q}_{\text{shift}_{[n]}} \right)^{-1} + \mathbf{H}_{[n]}^H \mathbf{R}_{[n]}^{-1} \mathbf{H}_{[n]} \right)}_{\text{inner Lyapunov operator}} \underbrace{\right)}_{\text{outer Lyapunov operator}}^{-1} \quad (58)$$

for general matrices $\mathbf{H}_{[n]}$ and $\mathbf{R}_{[n]}$. Then, it becomes clear that (58) consists of an inner and an outer Lyapunov style operators that interact, which essentially models two interacting systems of the from in (56). These dualities highlight an important issue. The Lyapunov and Riccati recursions used to model the involutions of physical systems are essentially representing the rotation, scaling, and shift, that these systems experience from one time instant to the next, which are more effectively dealt with using quaternions. Finally, the example given for a

scalar quaternion-valued random variable is extendable to higher dimensional systems. For more details on the use and behaviour of quaternion-valued Lyapunov and Riccati recursions, the reader is referred to [15,23].

SM-2: QUATERNION-VALUED MINIMUM MEAN SQUARE ERROR (MMSE) ESTIMATOR

Consider the MMSE estimator of a variable, y , conditioned on the observation, z , that is, $\hat{y} = E\{y|z\}$. For the case where y and z are quaternion-valued zero-mean and jointly Gaussian random variables, the MMSE estimator has to be expressed according to the real-valued components of the quaternion-valued random variables so that

$$\begin{aligned}\hat{y} = & E\{y_r|z_r, z_i, z_j, z_k\} + iE\{y_i|z_r, z_i, z_j, z_k\} + \\ & + jE\{y_j|z_r, z_i, z_j, z_k\} + \kappa E\{y_k|z_r, z_i, z_j, z_k\}\end{aligned}$$

whereby using (4) to replace $\{z_r, z_i, z_j, z_k\}$ with $\{z, z^i, z^j, z^k\}$ gives

$$\begin{aligned}\hat{y} = & E\{y_r|z, z^i, z^j, z^k\} + iE\{y_i|z, z^i, z^j, z^k\} \\ & + jE\{y_j|z, z^i, z^j, z^k\} + \kappa E\{y_k|z, z^i, z^j, z^k\}.\end{aligned}$$

Therefore, the MMSE solution in this case will take the form of an augmented estimator given by [17]

$$\hat{y} = \mathbf{g}^T \mathbf{z} + \mathbf{h}^T \mathbf{z}^i + \mathbf{u}^T \mathbf{z}^j + \mathbf{v}^T \mathbf{z}^k = [\mathbf{g}^T, \mathbf{h}^T, \mathbf{u}^T, \mathbf{v}^T] \mathbf{z}^a \quad (59)$$

where $\{\mathbf{g}, \mathbf{h}, \mathbf{u}, \mathbf{v}\}$ are quaternion-valued coefficient vectors and \mathbf{z} is the regressor vector. The estimator in (59) can also be expressed as

$$\hat{y}^a = \mathbf{W} \mathbf{z}^a \quad (60)$$

where \mathbf{W} is the matrix constructed appropriately from $\{\mathbf{g}, \mathbf{h}, \mathbf{u}, \mathbf{v}\}$ and their involutions [17].

SM-3: Relation Between the AQCF and Statistical Moments

Consider the AQCF in the formulation given in (9). Substituting the exponential with its power series representation yields

$$\begin{aligned}\Phi_{Q^a}(\mathbf{s}^a) = & E\left\{e^{\left(\frac{\xi}{4}\mathbf{s}^{aH}\mathbf{q}^a\right)}\right\} = E\left\{\sum_{m=0}^{\infty} \frac{\xi^m (\mathbf{s}^{aH}\mathbf{q}^a)^m}{(4^m)m!}\right\} \\ = & 1 + E\left\{\xi \frac{\mathbf{s}^{aH}\mathbf{q}^a}{4}\right\} - E\left\{\frac{(\mathbf{s}^{aH}\mathbf{q}^a)^2}{32}\right\} \dots\end{aligned} \quad (61)$$

Using the $\mathbb{H}\mathbb{R}$ -calculus and derivatives in (14) one can verify from (61) that

$$\begin{aligned} \frac{\partial \Phi_{Q^a}(\mathbf{s}^a)}{\partial \mathbf{s}^{*\zeta}} &= \frac{\partial \Phi_{Q^a}(\mathbf{s}^a)}{\partial \mathbf{s}^{aH} \mathbf{q}^a} \frac{\partial \mathbf{s}^{aH} \mathbf{q}^a}{\partial \mathbf{s}^{*\zeta}} = \mathbb{E} \left\{ \sum_{m=0}^{\infty} \frac{\xi^{m+1} (\mathbf{s}^{aH} \mathbf{q}^a)^m}{(4^{m+1})m!} \mathbf{q}^\zeta \right\} \\ &= \mathbb{E} \left\{ \xi \frac{\mathbf{q}^\zeta}{4} \right\} - E \left[\frac{\mathbf{s}^{aH} \mathbf{q}^a}{16} \mathbf{q}^\zeta \right] - \mathbb{E} \left\{ \xi \frac{(\mathbf{s}^{aH} \mathbf{q}^a)^2}{128} \mathbf{q}^\zeta \right\} \dots \end{aligned} \quad (62)$$

with $\zeta \in \{1, \iota, \jmath, \kappa\}$. Evaluating (62) at $\mathbf{s}^a = 0$ gives

$$\left. \frac{\partial \Phi_{Q^a}(\mathbf{s}^a)}{\partial \mathbf{s}^{*\zeta}} \right|_{\mathbf{s}^a=0} = \mathbb{E} \left\{ \xi \frac{\mathbf{q}^\zeta}{4} \right\}$$

and hence we have

$$\mathbb{E} \{ \mathbf{q} \} = \left(\frac{4}{\xi} \left. \frac{\partial \Phi_{Q^a}(\mathbf{s}^a)}{\partial \mathbf{s}^{*\zeta}} \right|_{\mathbf{s}^a=0} \right)^\zeta.$$

The second-order derivatives of Φ_{Q^a} can be expressed as

$$\frac{\partial^2 \Phi_{Q^a}(\mathbf{s}^a)}{\partial \mathbf{s}^{*\zeta_1} \partial \mathbf{s}^{*\zeta_2}} = \frac{\partial}{\partial \mathbf{s}^{*\zeta_1}} \left(\frac{\partial \Phi_{Q^a}(\mathbf{s}^a)}{\partial \mathbf{s}^{*\zeta_2}} \right) = \frac{\partial}{\partial \mathbf{s}^{aH} \mathbf{q}^a} \left(\frac{\partial \Phi_{Q^a}(\mathbf{s}^a)}{\partial \mathbf{s}^{aH} \mathbf{q}^a} \frac{\partial \mathbf{s}^{aH} \mathbf{q}^a}{\partial \mathbf{s}^{*\zeta_1}} \right) \frac{\partial \mathbf{s}^{aH} \mathbf{q}^a}{\partial \mathbf{s}^{*\zeta_2}} \quad (63)$$

where $\zeta_1, \zeta_2 \in \{1, \iota, \jmath, \kappa\}$. Upon replacing (62) into (63) we have

$$\frac{\partial^2 \Phi_{Q^a}(\mathbf{s}^a)}{\partial \mathbf{s}^{*\zeta_1} \partial \mathbf{s}^{*\zeta_2}} = \mathbb{E} \left\{ \sum_{m=0}^{\infty} \frac{-\xi^m (\mathbf{s}^{aH} \mathbf{q}^a)^m}{(4^{m+2})m!} \mathbf{q}^{\zeta_2} (\mathbf{q}^{\zeta_1})^\top \right\}$$

that evaluated at $\mathbf{s}^a = 0$ yields

$$\left. \frac{\partial^2 \Phi_{Q^a}(\mathbf{s}^a)}{\partial \mathbf{s}^{*\zeta_1} \partial \mathbf{s}^{*\zeta_2}} \right|_{\mathbf{s}^a=0} = \frac{-1}{16} \mathbb{E} \left\{ \mathbf{q}^{\zeta_2} (\mathbf{q}^{\zeta_1})^\top \right\}$$

giving the cross-correlation between \mathbf{q}^{ζ_1} and \mathbf{q}^{ζ_2} multiplied by the factor $(\xi/4)^2$. Note that all higher-order statistical moments of \mathbf{Q} are obtainable in an analogous manner.

SM-4: Real-Valued Components of (20)

Given $\{f(\cdot), g(\cdot)\} : \mathbb{H}^M \rightarrow \mathbb{H}$ the real-valued components of $h(\mathbf{q}) = f(\mathbf{q})g(\mathbf{q})$ are

$$\begin{aligned}\Re\{h(\mathbf{q})\} &= (\Re\{f(\mathbf{q})\})(\Re\{g(\mathbf{q})\}) + (\Im_i\{f(\mathbf{q})\})(\Im_j\{g(\mathbf{q})\}) \\ &\quad + (\Im_j\{f(\mathbf{q})\})(\Im_i\{g(\mathbf{q})\}) + (\Im_i\{f(\mathbf{q})\})(\Im_k\{g(\mathbf{q})\}) \\ \Im_i\{h(\mathbf{q})\} &= (\Re\{f(\mathbf{q})\})(\Im_i\{g(\mathbf{q})\}) + (\Im_i\{f(\mathbf{q})\})(\Re\{g(\mathbf{q})\}) \\ &\quad + (\Im_j\{f(\mathbf{q})\})(\Im_k\{g(\mathbf{q})\}) + (\Im_k\{f(\mathbf{q})\})(\Im_j\{g(\mathbf{q})\}) \\ \Im_j\{h(\mathbf{q})\} &= (\Re\{f(\mathbf{q})\})(\Im_j\{g(\mathbf{q})\}) + (\Im_i\{f(\mathbf{q})\})(\Im_k\{g(\mathbf{q})\}) \\ &\quad + (\Im_j\{f(\mathbf{q})\})(\Re\{g(\mathbf{q})\}) + (\Im_k\{f(\mathbf{q})\})(\Im_i\{g(\mathbf{q})\}) \\ \Im_k\{h(\mathbf{q})\} &= (\Re\{f(\mathbf{q})\})(\Im_k\{g(\mathbf{q})\}) + (\Im_i\{f(\mathbf{q})\})(\Im_j\{g(\mathbf{q})\}) \\ &\quad + (\Im_j\{f(\mathbf{q})\})(\Im_k\{g(\mathbf{q})\}) + (\Im_k\{f(\mathbf{q})\})(\Re\{g(\mathbf{q})\}).\end{aligned}$$

SM-5: Quaternion-Valued Least Mean Square Algorithm

Based on the regressor in (59), the aim is to find the weight vector \mathbf{w} so that the estimate $\hat{y}_n = \mathbf{w}_{[n]}^T \mathbf{z}_{[n]}^a$ tracks the observation sequence $\{y_{[n]} : n \in \mathbb{N}\}$ in a manner that minimises the cost

$$J_{[n]} = \|\epsilon_{[n]}\|^2 \quad \text{with} \quad \epsilon_{[n]} = y_{[n]} - \hat{y}_{[n]}.$$

This is performed in the least mean square (LMS) fashion via iterative updates of the weight vector as

$$\mathbf{w}_{[n+1]} = \mathbf{w}_{[n]} - \gamma \nabla_{\mathbf{w}^*} J_{[n]}$$

where $\gamma \in \mathbb{R}^+$ is an adaptation gain. Now, considering that $\|\epsilon_{[n]}\| \in \mathbb{R}$ and using the chain derivative rule of the $\mathbb{H}\mathbb{R}$ -calculus given in (27), we have

$$\nabla_{\mathbf{w}^*} J_{[n]} = \frac{\partial \|\epsilon_{[n]}\|^2}{\partial \|\epsilon_{[n]}\|} \nabla_{\mathbf{w}^*} \|\epsilon_{[n]}\| = -\frac{1}{2} \epsilon_{[n]} \mathbf{z}_{[n]}^{a*}.$$

Thus, the weight update term becomes

$$\mathbf{w}_{[n+1]} = \mathbf{w}_{[n]} + \gamma \epsilon_{[n]} \mathbf{z}_{[n]}^{a*} \tag{64}$$

with the $\frac{1}{2}$ factor absorbed into the adaptation gain.

Remark 8. Using the multiplication rule in (21), we can also have

$$\begin{aligned}\nabla_{\mathbf{w}^*} J_{[n]} &= \nabla_{\mathbf{w}^*} \|\epsilon_{[n]}\|^2 = \nabla_{\mathbf{w}^*} \left(\epsilon_{[n]}^* \epsilon_{[n]} \right) = \epsilon_{[n]}^* \left(\nabla_{\mathbf{w}^*} \epsilon_{[n]} \right) + \left(\nabla_{\mathbf{w}^*} \epsilon_{[n]}^* \epsilon_{[n]} \right) \epsilon_{[n]} \\ &= \frac{1}{2} \epsilon_{[n]}^* \mathbf{z}_{[n]}^{a*} - \mathbf{z}_{[n]}^{a*} \Re \{ \epsilon_{[n]} \} = -\frac{1}{2} \epsilon_{[n]} \mathbf{z}_{[n]}^{a*}.\end{aligned}\quad (65)$$

There are different derivations available, e.g., see [18,19,22]. Although these derivation might seem different from those in (64) and (65), they operate in the same manner.

Finally, if we assume that \mathbf{w}^{opt} exists so that $y_{[n]} = \mathbf{w}^{\text{opt}} \mathbf{z}_{[n]}^a$ and $\epsilon_{[n]} = \mathbf{w}^{\text{opt}} - \mathbf{w}_{[n]}$. Then, from (64) it follows that $\epsilon_{[n+1]}^H = \epsilon_{[n]}^H - \gamma \mathbf{z}_{[n]}^a \mathbf{z}_{[n]}^{aH} \epsilon_{[n]}^H$ which in turn yields the quaternion-valued Lyapunov function

$$\Sigma_{\epsilon_{[n+1]}^a} = (\mathbf{I} - \gamma \mathbf{G}_{[n]}) \Sigma_{\epsilon_{[n]}^a} (\mathbf{I} - \gamma \mathbf{G}_{[n]})^H$$

where $\Sigma_{\epsilon_{[n]}^a} = \mathbb{E} \{ \epsilon_{[n]}^a \epsilon_{[n]}^{aH} \}$, while

$$\Sigma_{\mathbf{z}_{[n]}^a} = \mathbb{E} \{ \mathbf{z}_{[n]}^a \mathbf{z}_{[n]}^{aH} \} \quad \text{and} \quad \mathbf{G}_{[n]} = \text{diag} \left\{ \Sigma_{\mathbf{z}_{[n]}^a}, \Sigma_{\mathbf{z}_{[n]}^a}^I, \Sigma_{\mathbf{z}_{[n]}^a}^J, \Sigma_{\mathbf{z}_{[n]}^a}^K \right\}.$$

Thus, if $\gamma < \mathbb{P} \{ \mathbf{G}_{[n]} \}$ and $\Sigma_{\mathbf{z}_{[n]}^a}$ is full rank; then, as $n \rightarrow \infty$ one has $\mathbb{P} \{ \Sigma_{\mathbf{z}_{[n]}^a} \} \rightarrow 0$, resulting in a convergent filtering operation.

SM-6: Quaternion-Valued Nonlinear Adaptive Filtering and Learning

Consider the operations of a computational element (neuron), formulated as

$$\hat{y}_n = h \left(\mathbf{w}_{[n]}^T \mathbf{z}_{[n]}^a \right)$$

where $\mathbf{z}_{[n]}$ is a vector presenting the inputs, $\mathbf{w}_{[n]}$ is a vector of the corresponding weights, and $h(\cdot) : \mathbb{H} \rightarrow \mathbb{H}$ is a differentiable function in \mathbb{H} . Note that for mathematical presentation the bias element is simply considered as an element of $\mathbf{z}_{[n]}$. The aim is to find optimal weight vector, \mathbf{w}^{opt} , so that the output, $\hat{y}_{[n]}$, is a close fit to desired output, $y_{[n]}$, in a manner that minimises a selected metric function $d(\cdot)$ so that $\{\mathbb{H}, d(\cdot)\}$ constitutes a convex metric space.

The weight vector is updated iteratively in order to reduce the cost

$$g(\mathbf{w}_{[n]}) = d(\hat{y}_{[n]} - y_{[n]}).$$

Specifically, we would like to achieve

$$g(\mathbf{w}_{[n+1]}) < g(\mathbf{w}_{[n]}) \quad (66)$$

with $\mathbf{w}_{[n+1]} = \mathbf{w}_{[n]} + \Delta\mathbf{w}_{[n]}$ where $\Delta\mathbf{w}_{[n]}$ represents a change in the weight vector from time instant n to time instant $n+1$. Taking the quaternion-valued Taylor series expansion of (66) yields

$$g(\mathbf{w}_{[n]}) + \left(\Delta\mathbf{w}_{[n]}^a\right)^H \nabla_{\mathbf{w}_{[n]}^{a*}} g(\mathbf{w}_{[n]}) + \mathcal{O}(g(\mathbf{w}_n)) < g(\mathbf{w}_n). \quad (67)$$

Neglecting the higher order terms in (67) gives $\left(\Delta\mathbf{w}_{[n]}^a\right)^H \nabla_{\mathbf{w}_{[n]}^{a*}} g(\mathbf{w}_{[n]}) < 0$. Therefore, considering $\Delta\mathbf{w}_{[n]}^a \propto \mu \nabla_{\mathbf{w}_{[n]}^{a*}} g(\mathbf{w}_{[n]})$ allows the formulation of a weight update procedure as

$$\mathbf{w}_{[n+1]}^a = \mathbf{w}_{[n]}^a - \gamma \nabla_{\mathbf{w}_{[n]}^{a*}} g(\mathbf{w}_{[n]}) \quad (68)$$

where $\gamma \in \mathbb{R}^+$ is an adaptation gain.

Remark 9. For the special case of $d(\cdot) = \|\cdot\|_2^2$ and using the Taylor series expansion of $g(\mathbf{w}_{[n+1]})$ around $\mathbf{w}_{[n]}$ suggests that $\gamma \in \left(0, \frac{1}{8\|\mathbf{z}_{[n]}^a\|_2^2 \|\nabla_{\mathbf{w}_{[n]}^{a*}} h(\mathbf{w}^T \mathbf{z}_{[n]}^a)\|_2^2}\right)$ ensures convergence.

SM-7: Distributed and Federated Learning

1-Distributed Estimation

In distributed estimation settings, multiple agents cooperate over an ad-hoc communication network in order to collaboratively estimate/track a state vector. In this setting, each agent implements a two stage learning process. First, a local estimate is formed using an agents own observations based on (36). Second, the agents fuse their local estimates with those of their neighbours using (44). This allows agents to learn from observations of other agents in the network, without the need for these observation to be shared. This scenario is shown in Fig. 3.

2-Federated Learning

One of the most popular multi-agent scenarios for learning from data sets that are distributed among a multitude of agents is federated learning. In its most fundamental level, at each time instant, agents (refereed to commonly as edge devices) that have new data sets available, update their estimate using (36), and then, send these updated estimates to a fusion centre which fuses these estimates with its existing information using (43). Then, the fusion centre pushes these unified estimates of the learnt parameters back to the agents. This scenario is shown in Fig. 4.

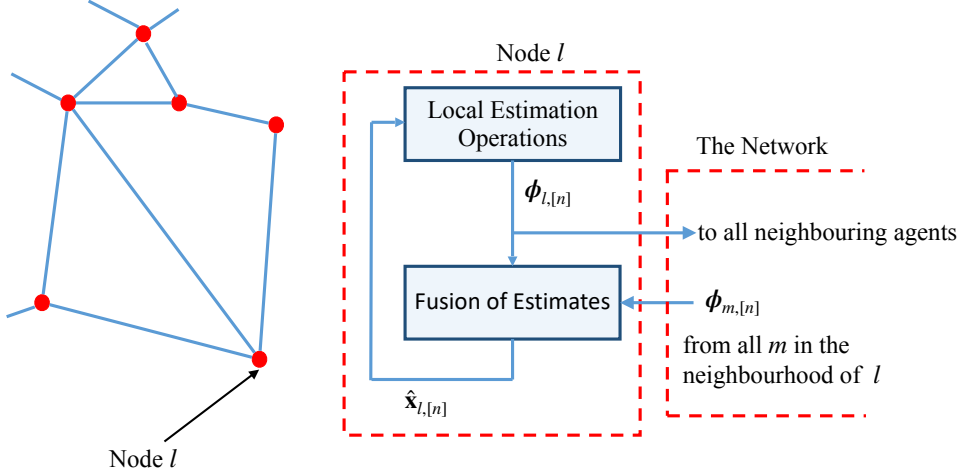


Fig. 3. Distributed learning scenario with a typical network shown on the left hand side and operations of an agent shown on the right hand side. The agent formulates and shares intermediate estimates $\psi_{l,[n]}$, while its fusion process produces estimates $\hat{x}_{l,[n]}$.

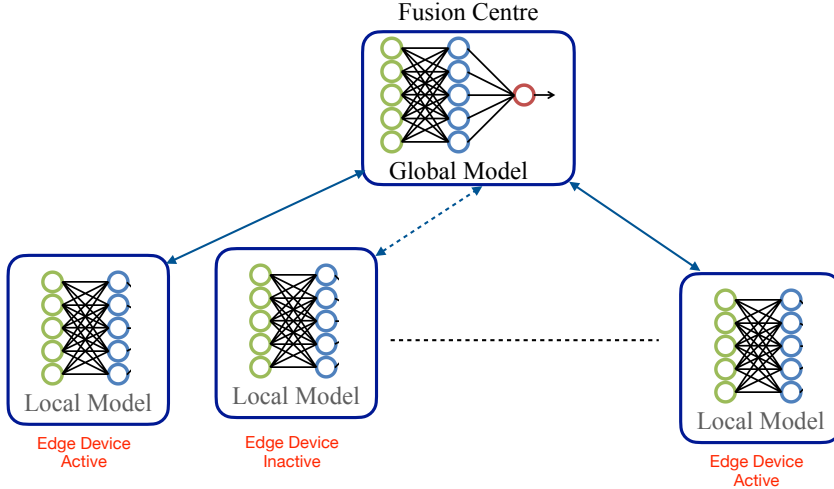


Fig. 4. The federated learning scenario is shown with a mix of active and inactive edge devices.

SM-8: Quaternion-Valued Hamilton-Jacobi-Bellman Type Recursion

The aim is to recover matrix sequence $\{\mathbf{P}_{[n]} : n \in \mathcal{N}\}$ that stratifies (50) and (51). For the case of $n = N$, from (50) it follows that $\mathbf{P}_{[N]} = \mathbf{T}$. Now, we assume that a positive definite Hermitian symmetric matrix $\mathbf{P}_{[n]}$ exist, so that $\mathcal{J}_{[n]} = \mathbf{x}_{[n]}^{aH} \mathbf{P}_{[n]} \mathbf{x}_{[n]}^a$. Then, for $\mathcal{J}_{[n-1]}$, we have

$$\mathcal{J}_{[n-1]} = \sum_{m=n-1}^N J_{[m]} = J_{[n-1]} + \underbrace{\sum_{m=n}^N J_{[m]}}_{\mathcal{J}_{[n]}} = \mathbf{x}_{[n-1]}^{aH} \Psi_{[n-1]} \mathbf{x}_{[n-1]}^a + \mathbf{x}_{[n]}^{aH} \mathbf{P}_{[n]}^a \mathbf{x}_{[n]}^a. \quad (69)$$

Substituting $\mathbf{x}_{[n]}^a$ from (47), into (69), we arrive at

$$\mathcal{J}_{[n-1]} = \mathbf{x}_{[n-1]}^{aH} \mathbf{P}_{[n-1]} \mathbf{x}_{[n-1]}^a \quad (70)$$

with

$$\mathbf{P}_{[n-1]} = \Psi_{[n-1]} + \left(\mathbf{A}^{a\mathsf{H}} + \mathbf{G}_{[n-1]}^{\mathsf{H}} \mathbf{B}^{\mathsf{H}} \right) \mathbf{P}_{[n]}^a \left(\mathbf{A}^a + \mathbf{B} \mathbf{G}_{[n-1]} \right).$$

Therefore, via induction, the expressions (69) and (70) show that there exists a positive definite matrix $\mathbf{P}_{[n-1]}$ so that $\mathcal{J}_{[n-1]} = \mathbf{x}_{[n-1]}^{a\mathsf{H}} \mathbf{P}_{[n-1]} \mathbf{x}_{[n-1]}^a$.

SM-9: Application Examples

A. Three-Phase Power Distribution Systems

The power grid is based on three-phase power production and distribution. To this end, instantaneous voltages can be combined into a quaternion signal

$$\begin{aligned} q_{[n]} = & iV_{a,[n]} \sin(2\pi f \Delta T n + \phi_{a,[n]}) + jV_{b,[n]} \sin\left(2\pi f \Delta T n + \phi_{b,[n]} + \frac{2\pi}{3}\right) \\ & + \kappa V_{c,[n]} \sin\left(2\pi f \Delta T n + \phi_{c,[n]} + \frac{4\pi}{3}\right) \end{aligned} \quad (71)$$

where $\{V_{a,[n]}, V_{b,[n]}, V_{c,[n]}\}$ (cf. $\{\phi_{a,[n]}, \phi_{b,[n]}, \phi_{c,[n]}\}$) are the instantaneous amplitudes (cf. instantaneous phases) on phase a , b , and c , while f is the system frequency⁵ and ΔT is the sampling interval.

For a three-phase power system operating under optimal (balanced) conditions, that is, $V_{a,[n]} = V_{b,[n]} = V_{c,[n]}$ and $\phi_{a,[n]} = \phi_{b,[n]} = \phi_{c,[n]}$, the system can be treated in the same manner as single phase operations. However, for a more general presentation and considering that all elements of (71) have the same frequency, it was shown in [15] that $q_{[n]}$ traces an ellipse in a plane of the three-dimensional imaginary subspace of \mathbb{H} . This is shown in Fig. 5, where the system voltages of a balanced and an unbalanced three-phase system are presented. Now, consider a new set of imaginary units, $\{\zeta, \zeta', \zeta''\}$ such that

$$\zeta \zeta' = \zeta'', \quad \zeta' \zeta'' = \zeta, \quad \zeta'' \zeta = \zeta' \quad (72)$$

and $\zeta - \zeta'$ reside in the same plane as $q_{[n]}$ (resulting in ζ'' being normal to the plane). An arbitrary ellipse in the $\zeta - \zeta'$ plane can then be expressed as

$$q_{[n]} = (A_{[n]} \sin(2\pi f \Delta T n + \phi_{\zeta,[n]}) + \zeta'' B_{[n]} \sin(2\pi f \Delta T n + \phi_{\zeta',[n]})) \zeta. \quad (73)$$

where $A_{[n]}, B_{[n]} \in \mathbb{R}$, are instantaneous amplitudes and $\phi_{\zeta,[n]}, \phi_{\zeta',[n]}$ are instantaneous phases. Replacing the $\sin(\cdot)$ and $\cos(\cdot)$ functions in (73) with their polar representations from (5) and

⁵Frequency is common among all phases due to structure of power generation systems.

after some mathematical manipulation, we have

$$q_{[n]} = \underbrace{\left(\frac{A_{[n]} e^{\zeta''(\phi_{\zeta, [n]})}}{2\zeta''} + \frac{B_{[n]} e^{\zeta''(\phi_{\zeta', [n]})}}{2} \right) e^{\zeta''(2\pi f \Delta T n)} \zeta}_{q_{[n]}^+} - \underbrace{\left(\frac{A_{[n]} e^{-\zeta''(\phi_{\zeta, [n]})}}{2\zeta''} + \frac{B_{[n]} e^{-\zeta''(\phi_{\zeta', [n]})}}{2} \right) e^{-\zeta''(2\pi f \Delta T n)} \zeta}_{q_{[n]}^-} \quad (74)$$

where

$$q_{[n]}^+ = e^{\zeta''(2\pi f \Delta T)} q_{[n-1]}^+ \quad \text{and} \quad q_{[n]}^- = e^{-\zeta''(2\pi f \Delta T)} q_{[n-1]}^-. \quad (75)$$

denote the two counter-rotating signals corresponding to the active and reactive elements of the power signal. These two counter rotating ellipses are shown in Fig. 6. Note that ideally, $q_{[n]}^- = 0$ with a signal only travelling in one direction (generation to consumption). From (75), state of the system is represented via the vector

$$\begin{bmatrix} \varphi_{[n+1]} \\ q_{[n+1]}^+ \\ q_{[n+1]}^- \end{bmatrix} = \begin{bmatrix} \varphi_{[n]} \\ \varphi_{[n]} q_{[n]}^+ \\ \varphi_{[n]}^* q_{[n]}^- \end{bmatrix} \quad (76)$$

where $\varphi_{[n]} = e^{\zeta'' 2\pi f_{[n]} \Delta T}$ with $f_{[n]}$ denoting the instantaneous frequency of the system. The quaternion model has two key advantages over its complex-valued duals. First, it allows to distinguish between different classes of faults [15]. Second, it produces estimates of system frequency with very low bias. This is demonstrated in Fig. 7, where state of the system is tracked using the derived model in (76) with frequency of the system is found from

$$\hat{f}_{[n]} = \frac{1}{2\pi\Delta T} \text{atan} \left(\frac{\|\Im(\hat{\varphi}_n)\|}{\Re(\hat{\varphi}_n)} \right). \quad (77)$$

Remark 10. The models in (74) and (75) have been used for analysis and fault detection in three-phase power systems [6,7,15,26,27].

B. Fly-by-Wire Flight Controller

In their most general formulation, the equation of motion governing the rotation of solid bodies can be summarised as

$$\frac{\partial \varphi}{\partial t} = \phi \quad \text{and} \quad \frac{\partial \phi}{\partial t} = \nu \quad (78)$$

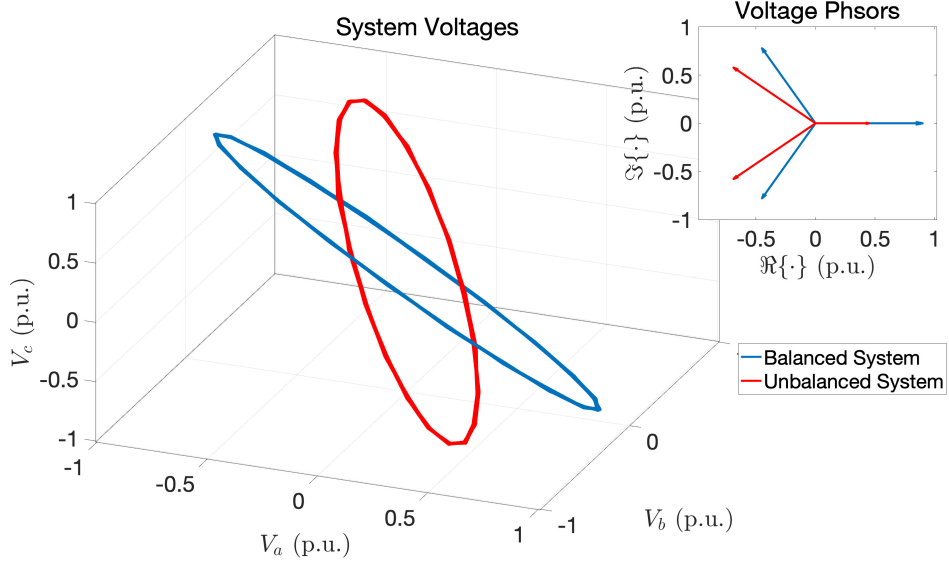


Fig. 5. Geometric view of the system voltages, $q_{[n]}$, and the corresponding phasor diagrams of a balanced and an unbalanced three-phase system. Note that p.u. stands for per unit.

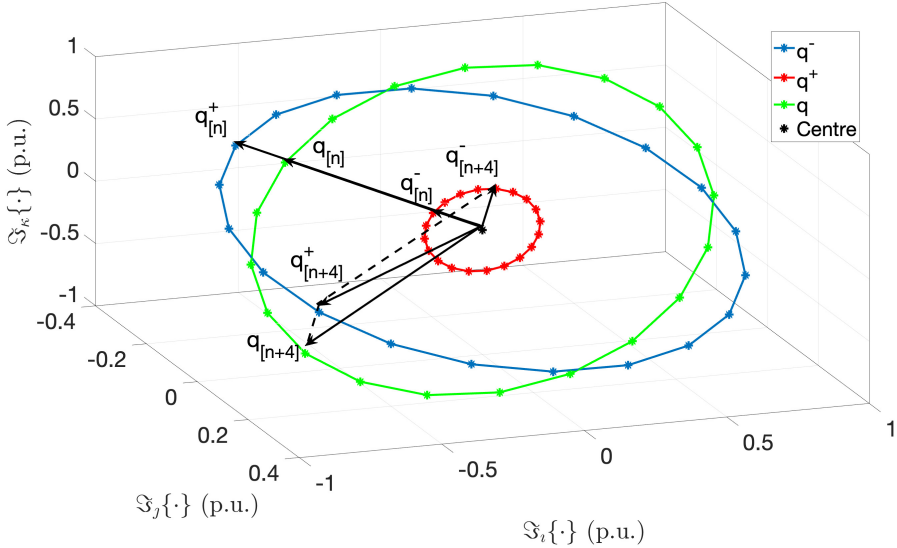


Fig. 6. System voltage, $q_{[n]}$, positive sequence element, $q_{[n]}^+$, and negative sequence element, $q_{[n]}^-$, of an unbalanced three-phase system suffering from an 80% drop in the amplitude of one phase and 20 degree shifts in the other phases. Note that p.u. stands for unit.

where ν represents the input to the system, typically torque or a related variable concerning angular acceleration), while φ represents the angular speed with $\dot{\varphi}$ indicating its rate of change. Transforming the equations in (78) into its discrete-time formulation yields

$$\begin{bmatrix} \varphi_{[n+1]} \\ \dot{\varphi}_{[n+1]} \end{bmatrix} = f \left(\begin{bmatrix} \varphi_{[n+1]} \\ \dot{\varphi}_{[n+1]} \end{bmatrix}, u_{[n]} \right) = \begin{bmatrix} 1 & \Delta T \\ 0 & 1 \end{bmatrix} \begin{bmatrix} \varphi_{[n]} \\ \dot{\varphi}_{[n]} \end{bmatrix} + \begin{bmatrix} \Delta T^2/2 \\ \Delta T \end{bmatrix} u_{[n]} \quad (79)$$

where $\Delta T = 0.04$ s denotes the sampling interval.

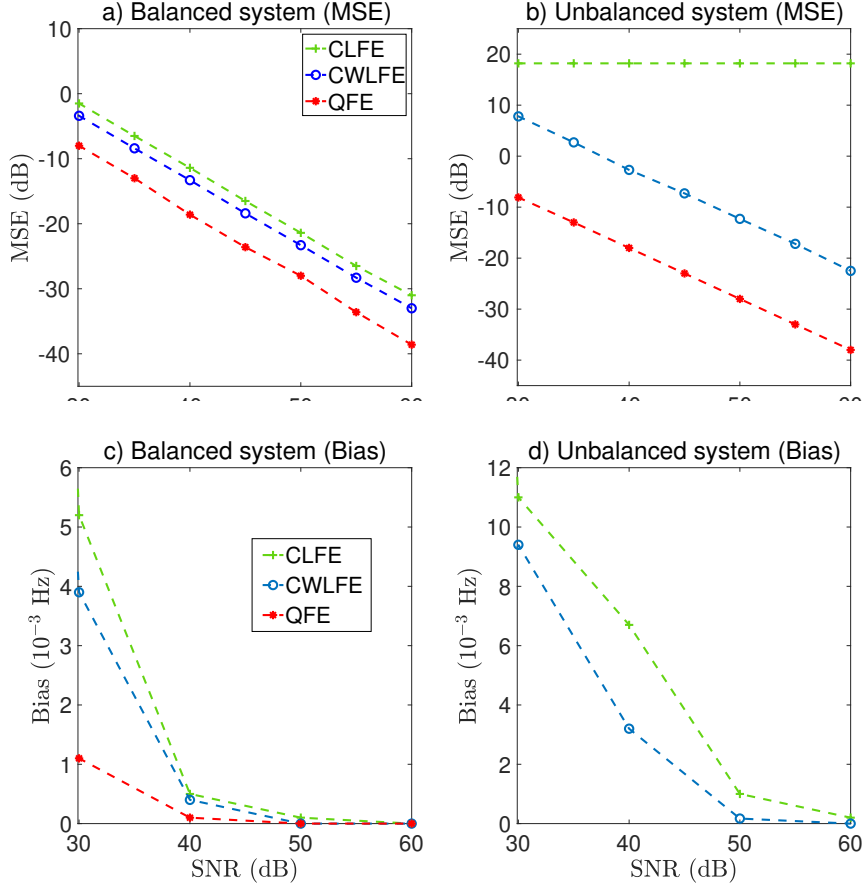


Fig. 7. Frequency estimation performance using the derived quaternion-valued model, quaternion frequency estimator (QFE), as compared to complex-valued linear (CLFE) and widely linear (CWLFE) techniques detailed in [15]; a) mean square error (MSE) performance for balanced system, b) MSE performance for the unbalanced system in Figure 6, c) bias performance for balanced system, and d) bias performance for the unbalanced system in Figure 6.

In order to present an illustrative example, consider the input, u_n , to be linear feedback regulator found via the framework in Section III-D, with

$$\mathbf{B} = \begin{bmatrix} \Delta T^2/2 \\ \Delta T \end{bmatrix} \text{ and } \mathbf{A} = \begin{bmatrix} 1 & \Delta T \\ 0 & 1 \end{bmatrix}$$

while $\mathbf{Q} = \mathbf{I}$, $\mathbf{T} = 50 \times \mathbf{I}$, and $\mathbf{R} = 10 \times \mathbf{I} - 1.875 \times (\mathbf{1}\mathbf{1}^\top)$. Inputs were calculated for 1.6 s long segments with the first half of the calculated sequences implemented. Then, input sequences were re-calculated using the new state-vector information. Fig. 8 shows the smooth trajectory of φ .

Remark 11. Note that quaternions have been an integral part of flight control systems [28]. Thus, this is not a novel application. However, quaternions have previously been decomposed into the real-part and a vector presenting the imaginary part. The advantage of the framework derived in this article is two-fold. First, the so-called augmented quaternion framework allows

useful tools from algebra, calculus, and statistics to be recovered in the quaternion domain. The section on calculus is addressed in this article, while [21] deals with quaternion statistics. Second, the approach presented in this article removes the need for transformations, under which the elegance, physical interpretation, and division algebra of quaternions is lost or obscured.

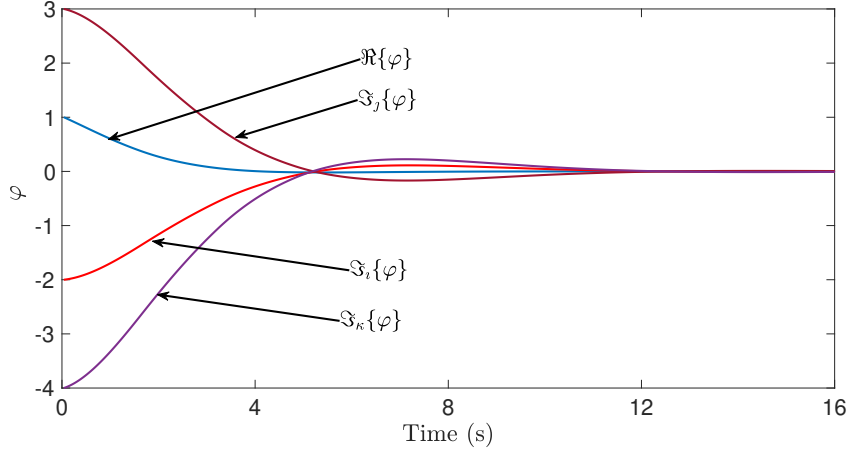


Fig. 8. Trajectory of φ under the proposed controller scheme.

C. Body Motion Tracking

The three Euler angles, as shown in Fig. 9, can be recorded using modern motion sensors. In order to make this data suitable for processing each angle was converted into a quaternion using the following transformations

$$\begin{aligned}\alpha &\rightarrow (\cos(\alpha), \sin(\alpha)) \rightarrow e^{i\frac{\alpha}{2}} \\ \beta &\rightarrow (\cos(\beta), \sin(\beta)) \rightarrow e^{j\frac{\beta}{2}} \\ \gamma &\rightarrow (\cos(\gamma), \sin(\gamma)) \rightarrow e^{k\frac{\gamma}{2}}\end{aligned}\tag{80}$$

with each term respectively representing the roll, pitch, and yaw rotations in the three-dimensional space. The three quaternion terms in (80) are now combined into one quaternion-valued variable given by

$$q = (e^{k\frac{\gamma}{2}})(e^{j\frac{\beta}{2}})(e^{i\frac{\alpha}{2}})\tag{81}$$

representing the overall rotation.

Remark 12. Note that since the mapping in (80) is invertible, the resulting quaternion-valued variable in (81) preserves dynamics of the signal.

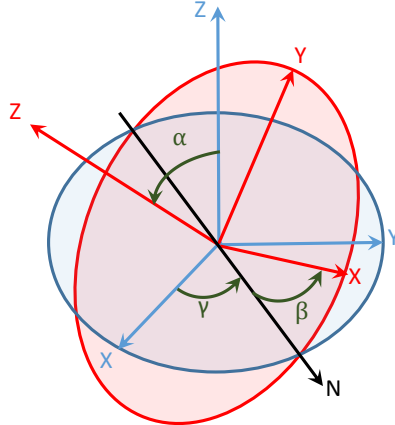


Fig. 9. Setting of the inertial body motion sensor with the fixed coordinate system (blue), sensor coordinate system (red), and Euler angles (green). The “N” axis is used as a visual guide to indicate the yaw angle. Figure taken from [15].

As an illustrative example, we recover the experiment in [15] using the frameworks in this article. Fig. 10 shows the recorded yaw angle measurements containing discontinuities and its corresponding continuous transformation in (80) which is ready for processing. The linear adaptive filter derived in SM-5 was considered in a one-step-ahead prediction setting to track body rotations. Fig. 11 shows the estimates of the absolute value of the phase for the body motion signal obtained by a quaternion-valued filter and its real-valued quadrivariate counterpart, that is, the case where quaternion-valued body motion signal was considered as a four-element vector with the real-valued least mean square (LMS) algorithm used to track the signal. Notice that the quaternion-valued filter had a significantly better performance than the quadrivariate LMS algorithm.

D. Bearings-only-Tracking

The problem of tracking the position of a manoeuvring target using sensors that can only measure the bearings of the target is considered. Commonly referred to as bearings-only-tracking, this problem is often encountered in passive radar, sonar, or infrared tracking applications. Since sensors can produce estimates of the target bearing and not of its range, none of the sensors can track the target location. Traditional solutions are based on congregating the information of all sensors at a central processing unit and resolving the location of the target through triangularisation. An elegant solution to this problem can be found via local fusion of sensor estimates over an ad-hoc network.

To this end, consider the target location at time instant n to be presented via the pure imaginary quaternion variable, $q_{[n]}$, in the manner given in Section I-C. Then, dynamics of

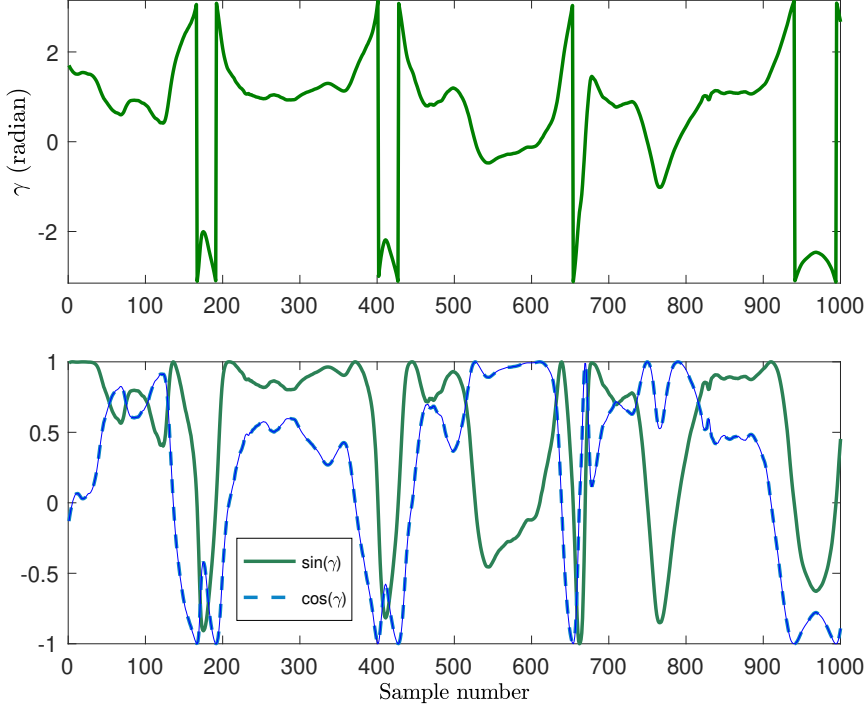


Fig. 10. Recorded yaw angle measurements with discontinuities at $\pm\pi$ (top) and its continuous transform (bottom).

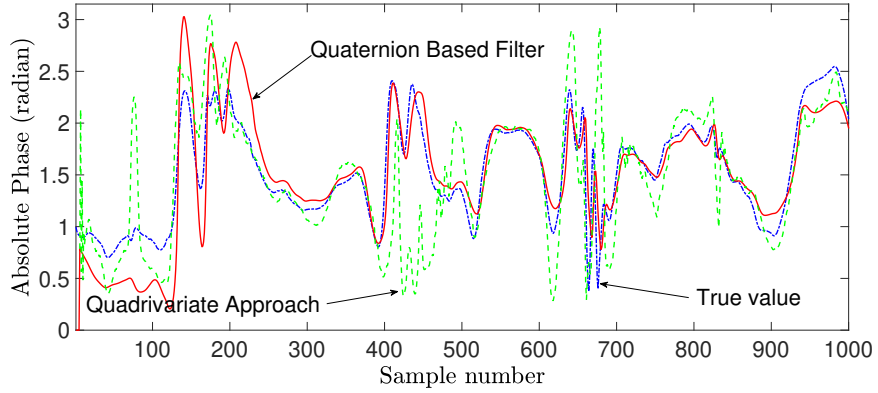


Fig. 11. Absolute value of the phase of quaternion-valued body motion signal employing the filter from SM-5 and a quadrivariate real-valued LMS approach.

the target can be formulated as

$$\begin{aligned} q_{[n+1]} &= q_{[n]} + v_{[n]} \Delta T + u_{[n]} \frac{1}{2} (\Delta T)^2 \\ v_{[n+1]} &= v_{[n]} + u_{[n]} \Delta T \end{aligned} \quad (82)$$

where $v_{[n]}$ and $u_{[n]}$ represent the speed and acceleration (normally modelled as zero-mean Gaussian noise) of the target, with ΔT representing the sampling interval. Moreover, sensor

l will have observations

$$y_{l,[n]} = \frac{q_{[n]} - L_{S_l}}{\|q_{[n]} - L_{S_l}\|} + w_{l,[n]} \quad (83)$$

where $w_{l,[n]}$ and L_{S_l} represent observation noise and location of sensor l .

As an illustrative example, the network shown in Fig. 12 with its nodes distributed uniformly inside a $24 \times 24 \times 24$ cube was used to track a target moving inside the cube through bearings-only measurements. The sampling interval was set to $\Delta T = 0.04$ s. The acceleration was considered as a zero-mean Gaussian noise sequence with independent components and variance of 10, while observation noise was considered to be zero-mean Gaussian with covariance of 10^{-4} and independent components. Agents used the framework derived in Section III-A to formulate a local estimates of the target which were then fused with those of the neighbouring agents via the framework of Section III-B. As a worst case scenario the tracking solution of the agent with only one connection is shown in Fig. 13. Note the accurate tracking solution achieved via the division algebra of quaternions. Although a similar approach can be implemented in vector algebras, the lack of division operation means normalisation and sensor fusion operations require more complex computations.

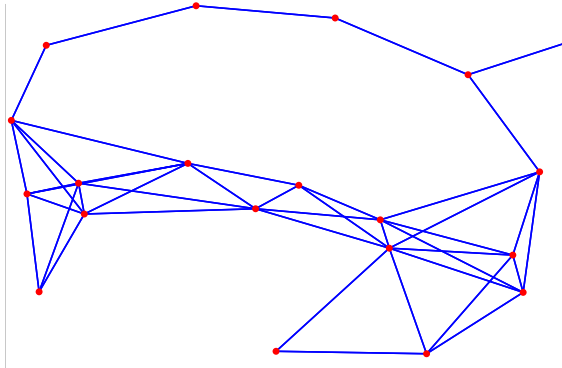


Fig. 12. Network of 20 nodes and 43 connections used in simulations.

E. Quantum Computing and the Compiler Problem

Recall the quaternion-valued model of a qubit given in Example 1. Although the model of a qubit with quaternions is not unique to that presented in this article. However, considering that the input and output of quantum computers are unit pure imaginary quaternions, the setting derived in this article allows all quantum computing operations to be modelled effectively using the division algebra of quaternions, e.g., involutions and rotations, operations. To this

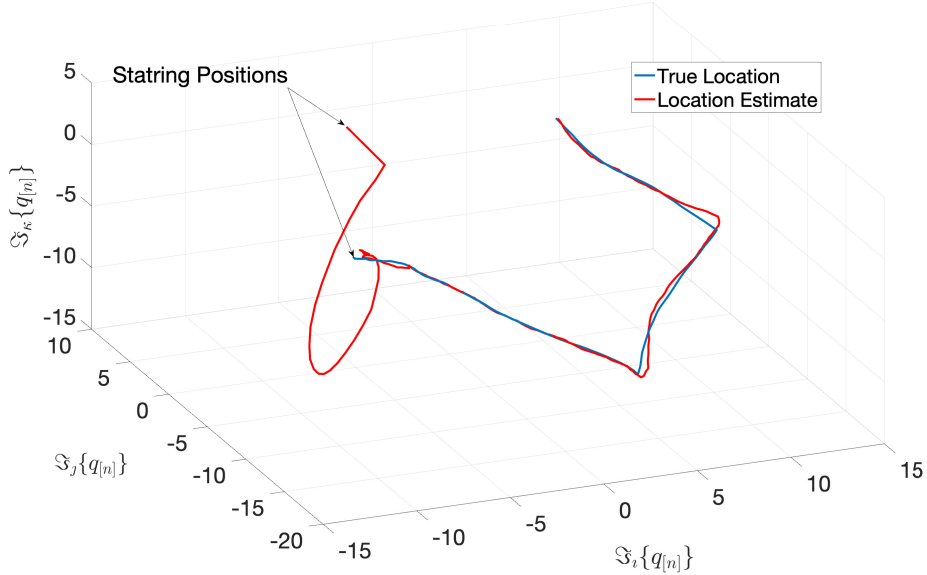


Fig. 13. Tracking solution of one agent in the bearings-only-tracking example.

end, consider the a general quantum computing operation represented by the mapping

$$\mathbf{q}_{\text{out}} \leftarrow f(\mathbf{q}_{\text{in}})$$

where $f(\cdot)$ is a quaternion-valued function. On the most general level, we would like to emulate this operation using a quantum computer the size and possible operations of which are represented as $\hat{\mathbf{q}}_{\text{out}} \leftarrow \hat{f}(\mathbf{q}_{\text{in}}, \mathbf{W})$ with \mathbf{W} denoting a parameter matrix with fixed values, representing fixed operations. This problem can be formulated as

$$\min_{\mathbf{W}} \left\{ \|f(\mathbf{q}_{\text{in}}) - \hat{f}(\mathbf{q}_{\text{in}}, \mathbf{W})\|^2 + g(\mathbf{W}) \right\} \quad (84)$$

$$\text{so that: } \mathbf{W} \in \mathcal{W} \quad (85)$$

where $g(\cdot) : \mathbb{H}^{M \times M} \rightarrow \mathbb{R}^+$ is a function representing the cost of implementing a certain structure and \mathcal{W} is the set of admissible values for \mathbf{W} . The solution to this problem has been considered in the form of factorisation and search algorithms [14]. These techniques, however, can be accelerated using the \mathbb{HR} -calculus, to indicate the steepest direction of reduction in cost. On a simpler level, the minima of (84) is calculable via gradient descent. This solution can then be projected to the closest $\mathbf{W} \in \mathcal{W}$ in order to meet the condition in (85).

Remark 13. The most important application of the setting derived in this article for modelling qubit is that it allows for most concepts in linear/nonlinear dynamic programming to be used in the context of quantum computing. Note that these concepts are expandable to the quaternion domain using the \mathbb{HR} -calculus.

Example 3. Quaternion-Valued Kalman Filtering

From Section III-A, let the evolution, observation, and metric functions be

$$\begin{aligned} f(\mathbf{x}_{[n]}, \mathbf{v}_{[n]}, \mathbf{u}_{[n]}) &= \mathbf{A}\mathbf{x}_{[n]}^a + \mathbf{B}\mathbf{u}_{[n]}^a + \mathbf{v}_{[n]}^a \\ h(\mathbf{x}_{[n]}, \mathbf{w}_{[n]}) &= \mathbf{H}\mathbf{x}_{[n]}^a + \mathbf{w}_{[n]}^a \\ d(\tilde{\epsilon}_{[n]}) &= 4\|\tilde{\epsilon}_{[n]}\|^2 = \text{tr}\left\{\tilde{\epsilon}_{[n]}^a \tilde{\epsilon}_{[n]}^{aH}\right\}. \end{aligned} \quad (37)$$

In this setting, from the framework of the $\mathbb{H}\mathbb{R}$ -calculus and (36), we have

$$\hat{\mathbf{x}}_{[n+1]}^a = \underbrace{\mathbf{A}\hat{\mathbf{x}}_{[n]}^a}_{\psi_{[n+1]}^a} + \mathbf{G}_{[n]} \begin{pmatrix} \mathbf{y}_{[n]} - \underbrace{\mathbf{H}\hat{\mathbf{x}}_{[n]}^a}_{\hat{\mathbf{y}}_{[n]}} \end{pmatrix}. \quad (38)$$

Using (37) and (38), the evolution of $\epsilon_{[n]}^a$ can be formulate as

$$\epsilon_{[n+1]}^a = (\mathbf{I} - \mathbf{G}_{[n]}\mathbf{H}) \mathbf{A}\epsilon_{[n]}^a + (\mathbf{I} - \mathbf{G}_{[n]}\mathbf{H}) \mathbf{v}_{[n]}^a + \mathbf{G}_n \mathbf{w}_{[n]}^a$$

which in turn yields

$$\begin{aligned} \epsilon_{[n+1]}^a \epsilon_{[n+1]}^{aH} &= (\mathbf{I} - \mathbf{G}_{[n]}\mathbf{H}) \mathbf{A}\epsilon_{[n]}^a \epsilon_{[n]}^{aH} \mathbf{A}^H (\mathbf{I} - \mathbf{G}_{[n]}\mathbf{H})^H \\ &\quad + (\mathbf{I} - \mathbf{G}_{[n]}\mathbf{H}) \mathbf{v}_{[n]}^a \mathbf{v}_{[n]}^{aH} (\mathbf{I} - \mathbf{G}_{[n]}\mathbf{H})^H + \mathbf{G}_n \mathbf{w}_{[n]}^a \mathbf{w}_{[n]}^{aH} \mathbf{G}_{[n]}^H. \end{aligned} \quad (39)$$

Taking the statistical expectation of (39) and solving for $\partial \mathbb{E}\{\epsilon_{[n]}\} / \partial \mathbf{G}_{[n]} = 0$ yields the optimal gain as

$$\mathbf{G}_{[n]} = \mathbf{M}_{[n]}\mathbf{H}^H \Sigma_{\mathbf{w}_{[n]}^a}^{-1} \quad (40)$$

where $\Sigma_{\mathbf{w}_{[n]}^a} = \mathbb{E}\{\mathbf{w}_{[n]}^a \mathbf{w}_{[n]}^{aH}\}$ and $\mathbf{M}_n = \mathbb{E}\{\epsilon_{[n]}^a \epsilon_{[n]}^{aH}\}$ are positive semi-definite matrices. Furthermore, replacing (40) into (39) gives the Riccati recursions

$$\mathbf{M}_{[n+1]} = \left(\left(\mathbf{A}\mathbf{M}_{[n]}\mathbf{A}^H + \Sigma_{\mathbf{v}_{[n]}^a} \right)^{-1} + \mathbf{H}^H \Sigma_{\mathbf{w}_{[n]}^a}^{-1} \mathbf{H} \right)^{-1}. \quad (41)$$

Note that (39) and (41) are Lyapunov and Riccati recursions that express how the elements of the error vector are expected to behave, that is, rotate and scale, that is *on par* with what is presented in SM-1. Finally, if $\{\mathbf{A}, \Sigma_{\mathbf{v}_{[n]}^a}^{\frac{1}{2}}\}$ (cf. $\{\mathbf{A}, \mathbf{H}\}$) are stabilisable (cf. detectable) in the isomorphic matrix algebra of quaternions (see SM-1 and [25]), for any positive definite initial matrix $\mathbf{M}_{[1]}$, (41) has a unique stabilising solution \mathbf{M} [23], which can be used for formulating a time-independent gain as, $\mathbf{G} = \mathbf{M}\mathbf{H}^H \Sigma_{\mathbf{w}_{[n]}^a}$ that guarantees $\rho\{(\mathbf{I} - \mathbf{G}_{[n]}\mathbf{H}) \mathbf{A}\} < 1$. For a detailed treatment of quaternion-valued Kalman filter the reader is referred to [15,23].